Water Balance Modelling for Reservoir Planning in Ribb Catchment, Ethiopia

Mecca Selman

March, 2009

Water Balance Modelling for Reservoir Planning in Ribb Catchment, Ethiopia

by

Mecca Selman

Thesis submitted to the International Institute for Geo-information Science and Earth Observation in partial fulfilment of the requirements for the degree of Master of Science in Geo-information Science and Earth Observation, Specialisation: (Integrated Watershed Modelling and Management)

Thesis Assessment Board

Dr. Ir. M.W. Lubczynski	(Chairman)	WREM dept., ITC, Enschede
Dr. Ir. J. Schellekens	(External examiner)	Deltaris, Delft
Dr. Ing. T.H.M. Rientjes	(First supervisor)	WREM dept., ITC, Enschede
Dr. A.S.M. Gieske	(Second supervisor)	WREM dept., ITC, Enschede

INTERNATIONAL INSTITUTE FOR GEO-INFORMATION SCIENCE AND EARTH OBSERVATION
ENSCHEDE, THE NETHERLANDS

Disclaimer

This document describes work undertaken as part of a programme of study at the International Institute for Geo-information Science and Earth Observation. All views and opinions expressed therein remain the sole responsibility of the author, and do not necessarily represent those of the institute.

DEDICATION

This little work is dedicated to my mother Zewdia Mussa

Abstract

The Ribb Reservoir is located East of Lake Tana in Amhara regional state 23km from Debre Tabor town in the North West part of Ethiopia. The geographical location of the reservoir at outlet is 12° 02’ 30”N 37° 59’ 45”E. The catchment including the reservoir covers a total area of 668km^2. Ribb reservoir is located in semi- arid region and suffers from water scarcity and due to this reason proper management for optimum use of the available fresh water resources is very crucial. The objective of this work is to assess the available water resources as it is the most important step towards proper management.

In this study, the components of water balance have therefore been assessed using a reservoir water balance method for the period 1997 to 2006.

For the case of runoff assessment per land cover unit, the catchment area has been classified into five land cover units (bareland, crops, forest, grassland and water) using Landsat images. The mean annual runoff from the catchment was estimated of 215 Mm^3. Runoff and rainfall are the two components constituting the total inflow to the reservoir. Irrigation water demand, evaporation and environmental flow are the outflow components of the reservoir.

Evaporation for open water is determined by Penman combination equation and precipitation is interpolated by inverse distance and Thiessen polygon weighting. Change in storage was calculated by determining all components of the reservoir. Catchment extraction was established from ASTER image elevation data and the catchment is divided in to three subbasins.

The HBV-96 model was applied to simulate the runoff from Ribb River using daily hydrometeorological data. The Nash-Sutcliff efficiency between observed and simulated of calibration and validation of the model shows that R^2 = 0.8 for calibration and R^2 = 0.81 for validation.

The storage capacity of the reservoir was estimated using ILWIS software through, trapezoidal and prismodal methods. Irrigation water demand was estimated by using CROPWAT for windows and environmental flow was determined by long-term monthly average flow of the river.

Acknowledgements

First and for the most praise to the almighty ALLAH who created and gave me the mind that can receive knowledge.

I would like to extend my sincere gratitude to my first supervisor, Dr. Ing. T. H. M. Rientjes, for his great insights, perspective, guidance and critical comments through out my thesis work. I learnt from him to understand what I read and how to reason out a research work. Our every fortnight group discussion has brought me to the compilation of my thesis within the allowed time. My sincere thanks also to my second supervisor Dr.A.S.M. Gieske for helping me in various ways to clarify the things related to my academic works in time with good cooperation and guidance. Beside the academic environment, I never forget the social life I enjoyed with him during my study here at ITC.

Thanks to the Directorate of ITC for providing me the scholarships and research Programs. I also thank my employer South Water Works Construction Enterprise for giving me a study leave to attend this MSc program. Sincere gratitude is also extended to the instructors in the department of water resources at ITC for their contribution to my study for eighteen months. I also wish to express my deepest thanks to those organizations Ministry of water Resources of Ethiopia and Ethiopian Meteorological Agency that provided me essential data for my study.

I would also like to express my appreciation to all WREM staff members and especially the program coordinator Ir. A.M. (Arno) van Lieshout for his valuable advice during my stay in ITC. In addition to this, I acknowledge to all WREM 2008 students for their pleasant and friendly discussion.

I feel a deep sense of gratitude for my father and mother who formed part of my vision and taught me the good things that really matter in life. I am grateful for my wife and my children and also my brothers for giving me the sense and the value of family life and brotherhood.

Table of contents

1. Introduction 1

1.1. Problem Statement 2
1.2. General Objective 2
1.3. Research Questions 3
1.4. Methodology 3
1.5. Literature Review 5
1.5.1. The Hydrologic Cycle 6
1.5.2. The Hydrological Model 7
1.5.3. The HBV Model 8
1.6. Thesis Structure 9

2. Study Area 11

2.1. Location 11
2.2. Topography and Drainage Network 12
2.3. Climate 14
2.4. Rainfall 14
2.5. Temperature 15
2.6. Hydrological Data 16
2.7. Evapotranspiration 17
2.8. Vegetation and Landcover 18
2.9. Geology 18

3. Reservoir Water Balance 19

3.1. Introduction 19
3.2. Data 19
3.3. Water Balance Analysis 20
3.3.1. Reservoir Water Balance Equation 20
3.3.2. Water Balance Components Derivation 21
3.3.3. Computation of Reservoir Capacity 25
3.3.4. Data Requirement 25
3.3.5. Area Volume Calculation 26
3.4. HBV Model 26
3.4.1. Background 26
3.4.2. Structure of the Model 27
3.4.3. Model Routine 29
3.4.4. Model Calibration 32
3.4.5. Setup of the Model 32
3.5. Irrigation and Crop Water Requirement 35
3.5.1. Crop Water Demand 36
3.5.2. CROPWAT 36
3.6. Environmental Water Flow 37

4. Results of Water Balance Components 39

4.1. Rainfall 39
4.2. Open Water Evaporation 39
4.3. Runoff 40
4.4. HBV Model 42
4.4.1. Data Input 42
4.4.2. Model calibration 42
4.4.3. HBV Model Validation 45
4.5. Storage Capacity 47
4.6. Irrigation Water Requirement 53
4.6.1. Crop Water Demand 55
4.6.2. Irrigable Area of the Study Area 57
4.7. Environmental Flow 59

5. Water Balance 61

5.1. Water Balance Components 61
5.2. Sensitivity Analysis 62

6. Conclusion and Recommendation 65

6.1. Conclusion 65
6.2. Recommendation 66

References: 67

Annex: 69

Appendix 1: Monthly Relative Humidity 69
Appendix 2: Monthly sunshine hours 69
Appendix 3: Monthly wind speed 70
Appendix 4: Monthly rainfall 70
Appendix 5: Monthly maximum temperature 71
Appendix 6: Monthly minimum temperature 71
Appendix 7: Contour lines at different elevation 72
Appendix 8: Photographs taken from the study area 73

List of figures

Figure 1-1: Flow chart of the methodology 4
Figure 1-2: Major processes of the schematized hydrologic cycle at a catchment scale 6
Figure 2-1: Location of the study area 11
Figure 2-2: Gradient to Upper Ribb from the source to the reservoir site and Lake Tana. 12
Figure 2-3: Digital elevation model of the Ribb catchment 13
Figure 2-4: Storage area and boundary of the reservoir catchment 13
Figure 2-5: Distribution of Annual Rainfall (1997-2007) 14
Figure 2-6: Distribution of monthly Rainfall (1997-2007) 15
Figure 2-7: Distribution of Daily Rainfall (1997-2007) 15
Figure 2-8: Distribution of maximum and minimum monthly temperature 16
Figure 2-9: Ribb river flow near Addis Zemen 16
Figure 2-10: Ribb river flow at reservoir site 17
Figure 2-11: Mean monthly evapotranspiration 17
Figure 2-12: Land cover map of Ribb catchment 18
Figure 3-1: Schematic representation of the reservoir water balance components 19
Figure 3-2: Locations of weather stations 21
Figure 3-3: Schematic representation of the HBV-96 model. 28
Figure 3-4: The soil moisture routine 30
Figure 3-5: The response routine 31
Figure 3-6: The transformation function 31
Figure 3-7: The flow chart of the HBV-96 model setup 33
Figure 3-8: Upper Ribb catchment divided into three subbasins 34
Figure 4-1: Rainfall results of the reservoir by Thiessen polygon and inverse distance weighting. 39
Figure 4-2: The relation of relative humidity, mean temperature, sunshine and evaporation. 40
Figure 4-3: Mean daily flow of Upper Ribb (m^3/s) during the wet year of 1998. 41
Figure 4-4: Mean daily flow of Upper Ribb (m^3/s) during dry year of 2001. 41
Figure 4-5: Scatter plot of calibration results 44
Figure 4-6: Simulated and observed hydrographs after model calibration 45
Figure 4-7: Scatter plot of validation results 46
Figure 4-8: Simulated and observed validation result 46
Figure 4-9: Contours generated from ASTER image for the reservoir 48
Figure 4-10: Area-volume relationship 50
Figure 4-11: Photographs taken from the study area at the reservoir site 51
Figure 4-12: Area-volume relationship 52
Figure 4-13: Comparison of volume in ILWIS calculation and contour calculation 53
Figure 4-14: Yearly inflow to the reservoir (1997-2006) 54
Figure 4-15: Mean monthly inflow to the reservoir (1997-2006) 54
Figure 4-16: Irrigable area with slope lower than 3% and larger than 0.2% 58
Figure 4-17: Irrigable area for gauged Ribb and total Ribb catchment 58
Figure 5-1: The water balance components of the reservoir 61
Figure 5-2: Sensitivity analysis of the reservoir 63

List of tables

Table 3-1: Weather data 20
Table 3-2: The three subbasins area: 33
Table 3-3: Subbasin area and landcover type 34
Table 3-4: The two station weights 34
Table 3-5: Parameters used for calibration 35
Table 4-1: Thiessen and inverse distance weights of Ribb reservoir 39
Table 4-2: Average annual river flow of upper Ribb 41
Table 4-3: Evapotranspiration weights of meteorological stations on the catchments 42
Table 4-4: Parameters used in HBV-96 model 43
Table 4-5: The objective function values obtained during the calibration process 44
Table 4-6: The objective function values obtained during the validation process 45
Table 4-7: Volume of the reservoir at each elevation by trapezoidal method 49
Table 4-8: Volume of the reservoir at each elevation by prismoidal method 50
Table 4-9: Volume of the reservoir at each elevation by ILWIS calculation 52
Table 4-10: Major crops, Kc value, ET_m and area weight of the crop 55
Table 4-11: ET_m calculation of selected crop 56
Table 4-12: Evaporation, Rainfall and Water demand for irrigation 56
Table 4-13: The water balance components and irrigable area 59
Table 4-14: Environmental flow for Ribb river 59
Table 5-1: The annual average water balance components of the reservoir 62

1. Introduction

Optimum and efficient use of scarce fresh water resources is becoming a prime concern these days as the disparity between the demands by ever increasing population to these precious resources is widening at an alarming rate. In arid and semi-arid areas recurrent drought and water shortage are common phenomenon. Thus, the competition over these resources is pronounced and sometimes leads to conflict among different users. In view of this an in-depth understanding of the hydrological behaviours of the catchment is necessary in the sense that it is an important step towards management of the water resources (Cherie Mekonnen, 2005). One way to acquire a better understanding is to use water balance modelling.

Ribb catchment is one of the agricultural areas of the country. However, this potential area is under threat. The ever-increasing devastation of the natural vegetation, the steep slopes, and traditional land management practices, poorly adapted to land conservation under the prevailing conditions, have resulted in dramatic soil erosion in the area.

In the past hundred years, the global population has tripled while demand for water has increased seven-fold (WWAP, 2003). The population in the area is expected to be triple over the next fifty years. This will place enormous additional pressure on the land base in the highlands, where it is already fully utilized. Indeed, it is clear that the land as a whole cannot possibly absorb the expected population, and alternate means of livelihood must be created.

Lake Tana's shore is characterized by flat low-lying land with poor drainage conditions. In these low-lying lands, the rivers have inadequate flood-carrying capacity due to mild slope and shallow cross-sections caused by sediment deposition in the riverbed. Surface inflows overtopping the riverbanks, direct rainfall on the area, poor drained soil and Lake Tana backwater effect also contribute to flooding in the area. This has even hampered the development of rainfed crops during the main season.

The introduction of irrigation will make farmers feel more secure about their basic food supply and enable them to diversify their crops based on local market demand and export opportunities. The land and water resources in the area are suitable for irrigation development. Experience from small-scale irrigation schemes has demonstrated that a range of crops could be grown profitably during the dry season, without affecting the production of staple food crops during the rainy season.

To enhance the economic viability of investments in infrastructure, it is important that irrigation developments focus on achievement of the benefits described above. The proposed reservoir allows development of tens of thousands of hectares of irrigated agriculture, thereby generating a demand for agricultural support services, and will enable farmers to fully benefit from more reliable access to sources of water.

Reservoir management involves allocating available water among multiple uses and users, minimizing the risks of water shortages and flooding and optimizing the beneficial use of water. Irrigation demands from a reservoir, which are generally computed by using the design cropping pattern and average rainfall conditions, may vary over the years depending on the actual cropping pattern and meteorological conditions (Goel et al., 2007). Optimization of irrigation systems for existing areas and improvement in water resource allocations by appropriate multi-cropping patterns and irrigation scheduling are the best response to reduce water deficits and to use available water. Irrigation scheduling deals with two basic questions: where and how much to irrigate. Because of an ever-increasing demand for irrigation water and the unreliability of stream flow in arid and semi-arid regions, performance evaluation of reservoir operation is important and particularly difficult. The most important aspect of operations is the release of the right quantity of water at the right time to irrigation areas to achieve greater benefits.

1.1. Problem Statement

Regarding the water resources management, there is increasing water utilization along the lower Nile valley straining the limited freshwater resources of the basin. Similarly, there is an increasing demand for irrigation and hydropower development in Ethiopia and the country is experiencing a number of problems such as rapid population growth, limited water resources, environmental degradation and poverty. Also it has to cope with recurrent droughts and increase agricultural production to balance with increasing population (Kebede et al., 2006).

Ribb is one of the catchments of Lake Tana basin located in the eastern part of the basin that is affected by annual flooding. This flood affects inhabitants by flooding agricultural lands during the wet season and the flood indicated that the Ribb river is flowing bank full at the bridge, while upstream the river was overflowing at the confluence with the Sheni river. This flood water discharged into the Fogera plain. Overflow is caused in rainy seasons due to the rain falling upstream in the catchment in combination with the obstruction of the bridge. However, it is likely that the Ribb river also spills upstream of the gauging site and this spill drains via the road culverts towards the flood plain. Controlling the flood and managing the incoming water is a crucial issue, as there is a continuously growing demand for water for various purposes during the year.

1.2. General Objective

To quantify water balance components of the Ribb reservoir for flood protection and irrigation by using water balance modelling.

Specific objectives

- To asses the rainfall-runoff relation of the catchment
- To identify possible water demands of the reservoir
- To define the required storage capacity of the reservoir

1.3. Research Questions

- What are the water balance components at the reservoir to be established?
- Could reservoir building reduce downstream flooding in Fogera flood plain?
- What maximum and minimum storage volume of reservoir is required?

1.4. Methodology

The study is carried out in three main stages, they are:

Pre-field work

This involves problem definition, literature review, identifying data required for modelling, collection of available data from ITC data base and acquiring necessary images from various sources.

Field work

This involves collection of hydrological and meteorological data from concerned offices and collection of observed data.

Post-field work

This involves arranging and preparing data for the model processing and analyzing, water balance model development, writing thesis work and preparation for presentation. Figure 1-1 shows a flow chart of the methodology adopted for this work.

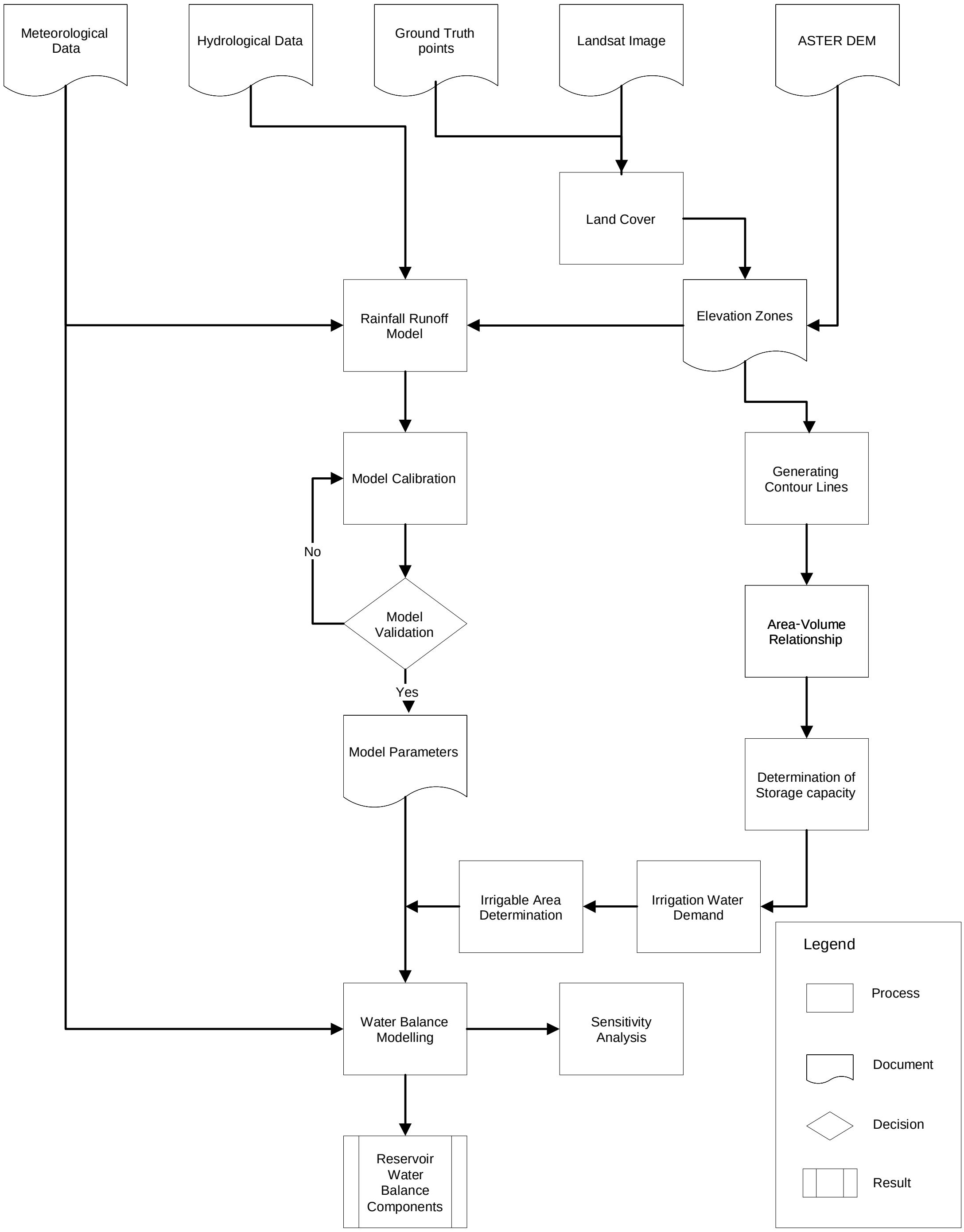

Figure 1-1: Flow chart of the methodology

1.5. Literature Review

Uncertainties in water balance estimates

The water balance estimates of a catchment or a reservoir involves different parameters and variables recorded in hydrometeorological stations and some times obtained from model calibrations. Human or instrumental errors are associated with such estimates. A comprehensive analysis with regard to uncertainties in estimating the water balance of lakes (reservoirs) is presented by Winter (1981). Forexample, estimates of precipitation can have a wide range of error, depending on the gage placement, gage spacing, and areal averaging technique. Errors in measurement of individual storms can be as high as 75 percent. Errors in short term averages are commonly in the 15-30 percent range, but decrease to about 5 percent or less for annual estimates. Errors in estimates of evaporation can also vary widely depending on instrumentation and methodology. The energy budget is the most accurate method of calculating evaporation; errors are in the 10-15 percent range. Clearly these errors also propagate with the modeling of the rainfall-runoff relationship.

Effect of land use change on hydrology

Land use changes that could have an effect on decrease or increase of the quantity of water input to the Ribb reservoir is selected from Maidment's expanded description Maidment (1993).
In the same source impacts of Urbanization on storm water runoff are discussed and commonly urbanization increases surface storm runoff and modifies its quality. As land urbanizes, it is covered by impervious surfaces such as paved roads, parking lots and roofs which prevent rainfall or snowmelt from infiltrating into the ground.

A change in land use is likely to alter the availability of water at the evaporating surface through changes in:

- The surface area of free water surfaces in streams and lakes(reservoirs)
- The availability of soil water to plants (for example, when short-rooted agricultural crops replace deep-rooted trees, the availability of water will be reduced in dry periods or when drainage reduces soil moisture content in the rooting zone)
- Replacement of crops with different total leaf area per unit ground area (leaf area index, LAI), different stomatal resistance, and different stomatal responses to soil water and atmospheric humidity deficits.

A model for predicting the effects of a land-use change should have:

- Input data requirements which can be satisfied
- A range of application which covers the problem being considered
- Sufficient complexity to give the required prediction accuracy- uses the simplest model which will give a sufficiently accurate result (Maidment, 1993).

1.5.1. The Hydrologic Cycle

As indicated in most of hydrology literatures the continuous movement of all forms of water on the earth is called hydrologic cycle. This includes condensation of vapour in the atmosphere that gives rise to precipitation. Precipitation partly intercepts by vegetation and partly reaches the surface. Evaporation takes place from the intercepted water by vegetation and from the surface storage. Water also flows through streams and reach lakes and reservoirs from where evaporation and seepage to groundwater occurs. Precipitation that infiltrates in to the soil could also leave by evapotranspiration or reach streams by through flow and partly percolates to groundwater. The depletion of water in the surface and subsurface due to evaporation and evapotranspiration causes groundwater to move upward direction through the process called capillary rise. Some of it evaporates or moves to streams as base flow or to the oceans and lakes through deeper routes (Gebreegziabher, 2005).

Unsaturated flow, macro pore flow and perched flow perform due to the contribution of precipitation. The process of percolation will occur when the unsaturated flow recharges the ground water. Macro pore and perched flow allow to pass the water and this water will recharge the groundwater flow and cause a rise of the water table. Percolation is a process when rainwater reaches groundwater and this groundwater distributed in to channel flow which is base flow and evaporation. But, inmost cases most part of the groundwater will be as ground water or it contributes to ground water storage. In general evaporation is defined as the aggregation of evaporation from canopy, plant transpiration, evaporation from the soil and free water evaporation. Groundwater is the contribution of catchment runoff and channel flow will contribute to catchment runoff.

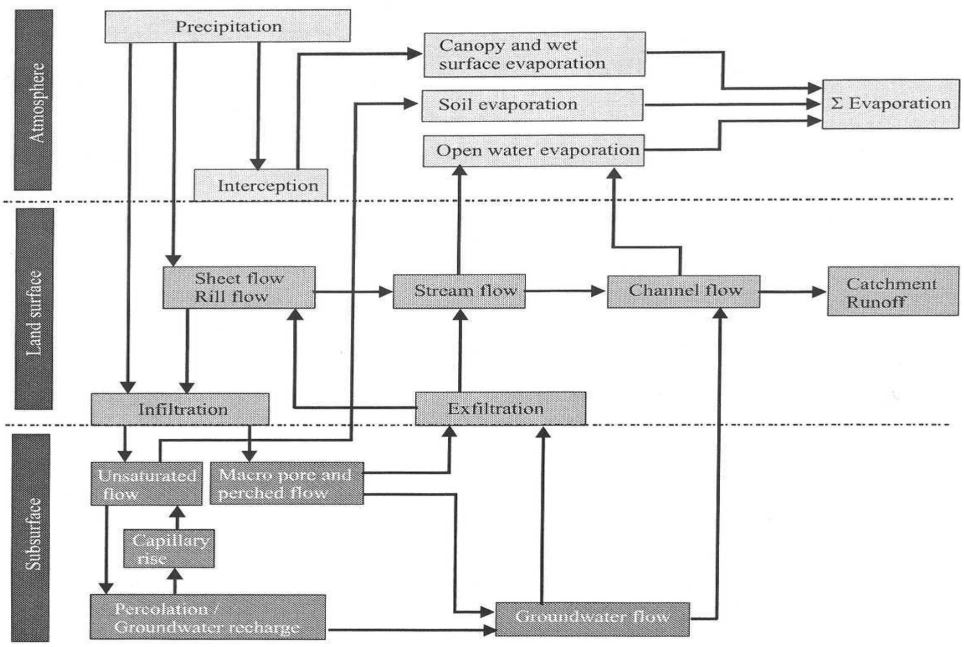

Figure 1-2: Major processes of the schematized hydrologic cycle at a catchment scale
Source: Rientjes (2007)

1.5.2. The Hydrological Model

Use of hydrological Modelling

Hydrological models are mathematical formulations which determine the runoff signal which leaves a watershed basin from the rainfall signal received by this basin. They provide a means of quantitative prediction of catchment runoff that may be required for efficient management of water resources. Such hydrological models are also used as means of extrapolating from those available measurements in both space and time into the future to assess the likely impact of future hydrological change. Changes in global climate are believed to have significant impacts on local hydrological regimes, such as in stream flows which support aquatic ecosystem, navigation, hydropower, irrigation system, etc. In addition to the possible changes in total volume of flow, there may also be significant changes in frequency and severity of floods and droughts.

Runoff generation processes are often poorly understood at a catchment scale before an experimental investigation is carried out. Rainfall runoff models have improved in the recent years. Increased computer capacities have made it possible to develop distributed physically based models. However, the enormous data requirements prevent the extensive use of these models. Conceptual models are less complex, relatively easy to use and the required input data are available for most applications. But there exists a large model uncertainty (Grayson et al., 1992) and a parameter uncertainty (different parameter sets reach equally good simulation results). In addition, most parameters have to be determined by calibration and cannot be derived from basin characteristics. This causes uncertainties of the discharge simulation, which are enlarged if the uncertainties of the input data are considered (Uhlenbrook and Leibundgut, 2000).

Hydrological models that simulate the hydrological response caused by these changes in land cover are traditionally based on soil moisture accounting and routing, with a simple cause-effect relationship in precipitation-runoff generation. State of the art models also tend to be over parameterised leading to shortcomings in describing the catchment hydrological response.

The HBV-96 model is selected for this study because of the following reason:

- the input data requirement is moderate
- the model simulates the major hydrological process in a catchment
- the model was tested for water balance modelling in different parts of the world
- the availability of the model

1.5.3. The HBV Model

The HBV-96 model is a conceptual hydrological model for continuous simulation of runoff. It was originally developed at the Swedish Meteorological and Hydrological Institute (SMHI) in the early 1970s. Since then the model has found application in more than 40 countries. Originally the HBV-96 model was developed for runoff simulation and hydrological forecasting, but the scope of the application has increased steadily. Today the HBV-96 model can be used (Seibert, 2002):

- for water balance studies
- for runoff forecasting (flood warning and reservoir operation)
- to compute design floods for dam safety
- to investigate the effects of changes with in the catchment
- to simulate climate change effects

In 1993 the Swedish Association of River Regulation Enterprises (VASO) and SMHI initiated a major revision of the structure of the HBV-96 model with the same philosophy of simplicity as the original HBV-96 model to make the model more physically reasonable and up-to-date with the current hydrological and meteorological knowledge. HBV-96 is the final result of this model revision.

The HBV-96 is best described as a semi-distributed conceptual model. The model simulates daily discharge using daily rainfall, temperature and estimates of potential evapotranspiration as input together with geographic information about the river catchment. The evapotranspiration values used are long-term monthly averages. Discharge observations are used to calibrate the model, and to verify and correct the model before a runoff forecast. The model consists of subroutines for snow accumulation and melt, soil moisture accounting, runoff generation and finally, a simple river flow routing procedure.

It is possible to run the model separately for several subbasins and then add the contributions from all subbasins. Calibration as well as forecasts can be made for each subbasin. For basin of considerable elevation range a subdivision into elevation zones can be made. Each elevation zone can further be divided into different vegetation zones (forested and non-forested areas).

1.6. Thesis Structure

This work which includes the introductory chapter has been developed to have totally six chapters. The general description of each chapter mentioned as follows:

Chapter 1: Describes introduction to the thesis, general objective of the study, the research questions and Literature review.

Chapter 2: General description and Location of the study area, this includes rainfall, climate, topography and drainage network, catchment Hydrology and Land cover.

Chapter 3: Explains: The reservoir water balance components and the methodology of the study followed for determination of storage capacity and derivation of water balance components.

Chapter 4: Deals with: Data processing and results of water balance components such as evaporation, rainfall, irrigation water demand and Environmental flow.

Chapter 5: It incorporates the results of water balance model components.

Chapter 6: The last chapter includes conclusion and Recommendation

2. Study Area

2.1. Location

Ribb dam site is located on the Ribb river on the eastern side of Lake Tana Basin, in the South Gondar Zone of Amhara National Regional State (See Fig. 2-1)

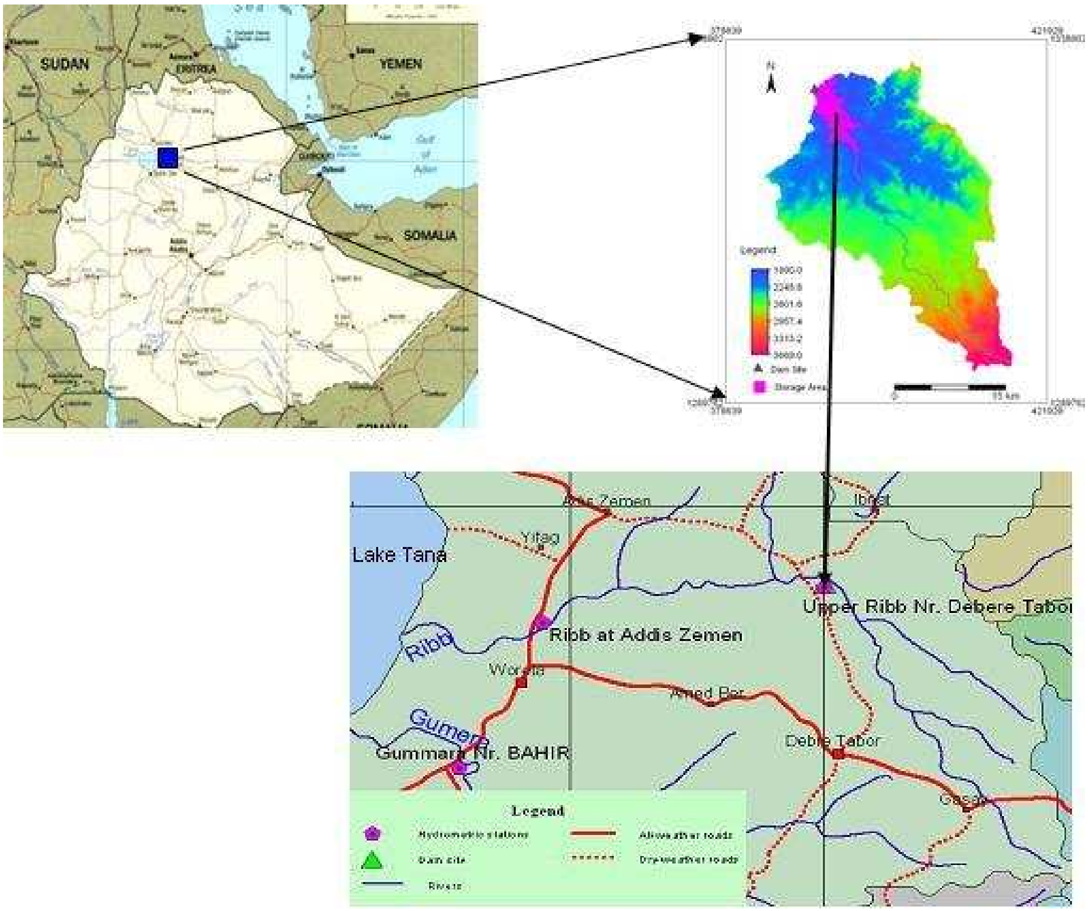

Figure 2-1: Location of the study area

The riverbed elevation at the reservoir axis is about 1,870 m at coordinates and 12° 02’ 30”N 37° 59’ 45”E. Approximate longitudinal section of the Ribb watershed along the main river course shows that it is characterized as a steep mountainous watershed up to the Ribb dam site, below this point the river slope is getting flatter (Figure 2-2).

The Upper Ribb watershed is characterized as a mountainous, wedge shaped and a steep sloped watershed Figure 2-2. The highest elevation of the watershed is about 4,100 m in the south eastern part, where at the reservoir site the elevation drops below 1,900 m. Debre Tabor, Ibnat and Gasay towns are located on the divide line, near, and inside the Upper Ribb watershed, respectively.

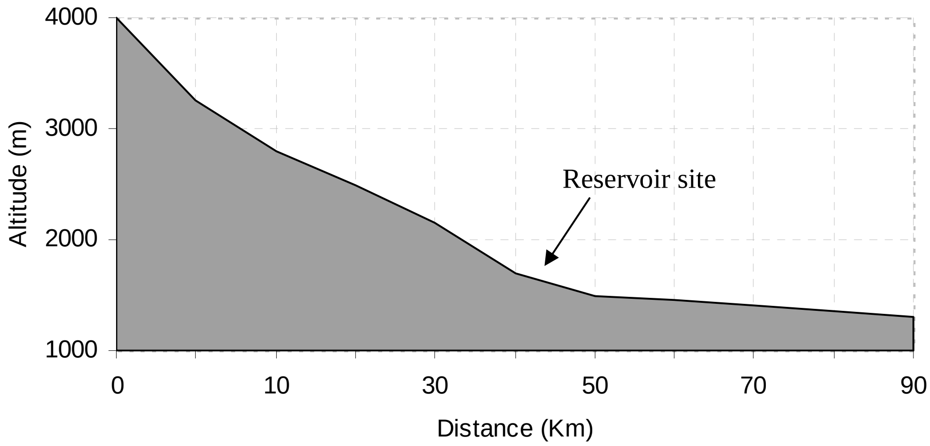

Figure 2-2: Gradient to Upper Ribb from the source to the reservoir site and Lake Tana.

The Ribb River, which is some 130 km long, has catchment area at the reservoir site of 668 km^2. The river, which flows generally in a westerly direction and dins into Lake Tana, is one of the main streams flowing into Lake Tana from the east. The Ribb River, with its tributaries, drains the western slope of the high mountainous area east of the town of Debre Tabor. In the low and middle reaches of the river, especially in the extensive alluvial plains bordering the lake, the river meanders its way and flows slowly, causing serious river channel deposit, high water table and overflow of riverbanks during the rainy season. Consequently, major problems of flooding and water logging must be resolved in order to develop irrigated agriculture in the area.

2.2. Topography and Drainage Network

The reservoir site is characterized by broad and flat flood plains, old bench forming terrace and low to high relief basaltic hills with steep to moderately steep slopes. There are developments of relatively few shallow seated gullies at the reservoir catchments attributed to rill and gully erosion. The peak topography in the reservoir area is marked by Shikra Hill, which is at an altitude of 1973 m. The Upper Ribb watershed is characterized as a mountainous, wedge-shaped and steep-sloped watershed. The highest elevation of the watershed is about 4,100 m in its south eastern part. The lowest topography land is at the dam site, which is at an altitude of 1870m.

In general the study area has a topography ranging from nearly flat to high sloping. Figure 2-3 below shows the digital elevation model of the study area generated from Aster image. The Aster image obtained from USGS has 30m resolution. The average elevation of the catchment area is 1926m with minimum and maximum elevations of 1780 m and 4100 m above sea level, respectively.

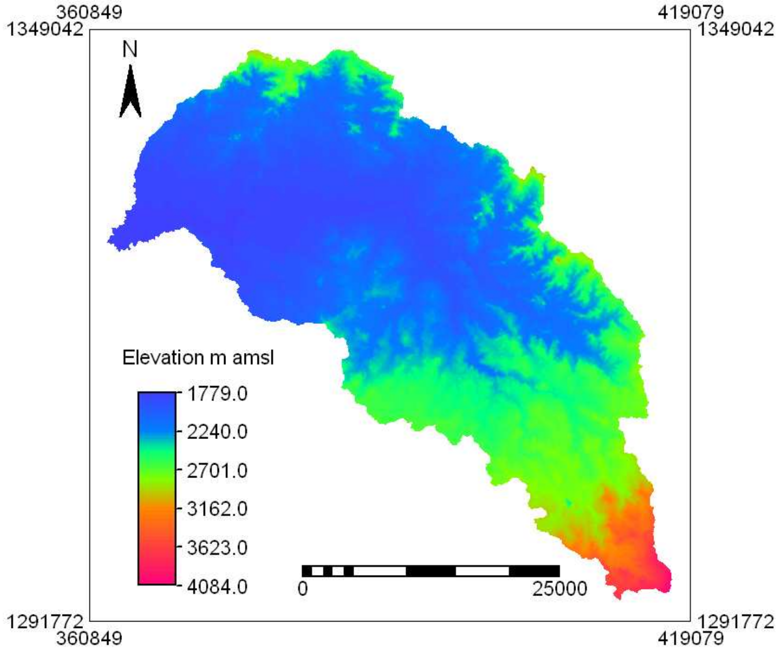

Figure 2-3: Digital elevation model of the Ribb catchment

Upper Ribb watershed (that includes the Ribb dam site watershed) is highly vulnerable to sheet, rill and gully erosions. Mean annual rainfall over the Ribb dam site watershed is larger than 1,400 mm and 56 km downstream of the Upper Ribb gauging site, the Ribb river slope is getting flatter with low flow velocity and deposition of suspended sediment in the river course and over the banks in case of excessive flooding.

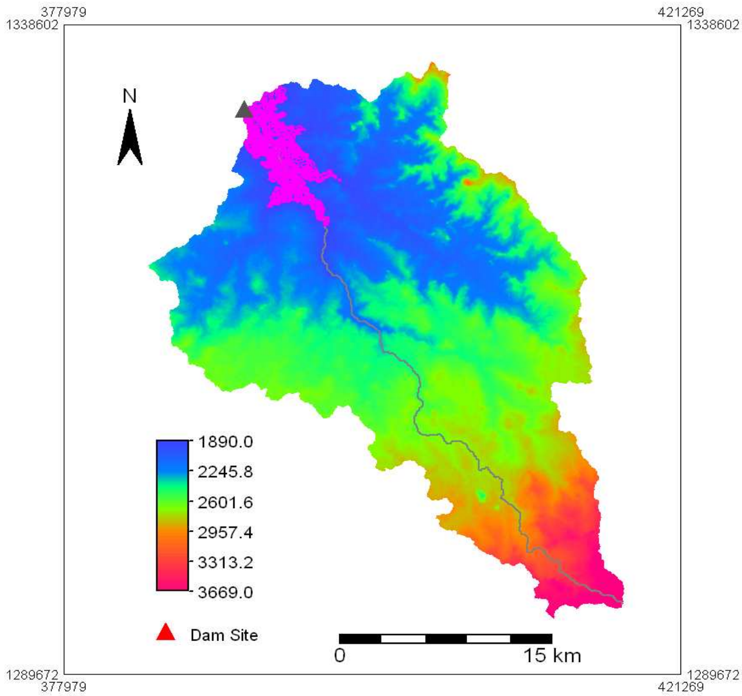

Figure 2-4: Storage area and boundary of the reservoir catchment

2.3. Climate

The climate of the Ribb Basin is marked by a rainy season from June to September, with monthly rainfall varying from 65 mm in May to 411 mm in July. Mean annual precipitation is about 1,500 mm in the upper part and about 1,200 mm in the lower part. The dry season, from October to April, has a total rainfall of about 8% of the mean annual rainfall. Dependable rainfall varies from less than 13 mm during the dry season to 80–275 mm/month during the period of June to July/August, equivalent to 40–80% of the average values. Temperature variations throughout the year are minor (19 ºC in December to 23 ºC in May), with maximum and minimum temperatures of 30 °C and 11.5 °C, respectively. Humidity varies between 70% in Dec and 88% in August. Wind speed is low, thus minimizing potential evapotranspiration values between 95 mm/month in December and 140 mm/month in April. Sunshine duration is reduced to 6.0–6.5 hours during July and August.

2.4. Rainfall

The mean annual rainfall of the area calculated using the daily long-term rainfall record of Debre Tabor station is 1500 mm. As shown in Figure 2-5 the annual rainfall doesn’t have high degree of variation. The wettest year in the record period is 2000 with rainfall of 1631mm and the amount recorded in the driest year 1998 and 2001 was 1145mm and 1149mm respectively.

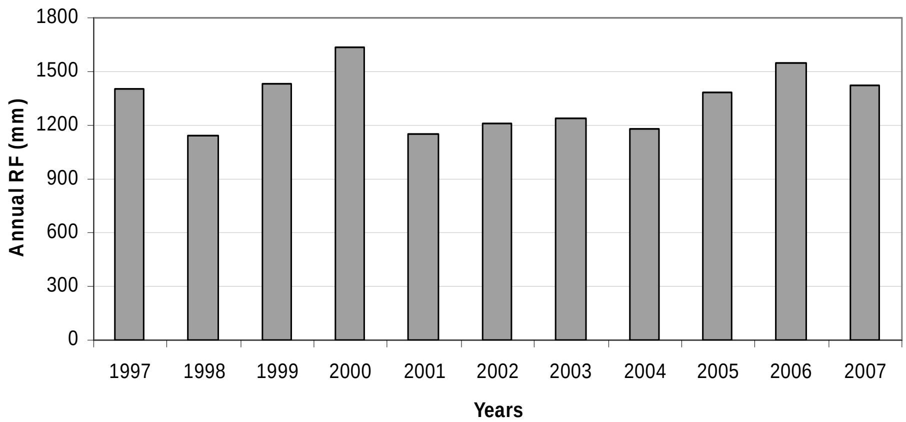

Figure 2-5: Distribution of Annual Rainfall (1997-2007)

The wet period in a year lies between June to September with maximum rainfall in July of 416mm. The dry period lies between November to February and the minimum rainfall in February. Ninety percent of the mean annual rainfall is observed in the period from June through September.

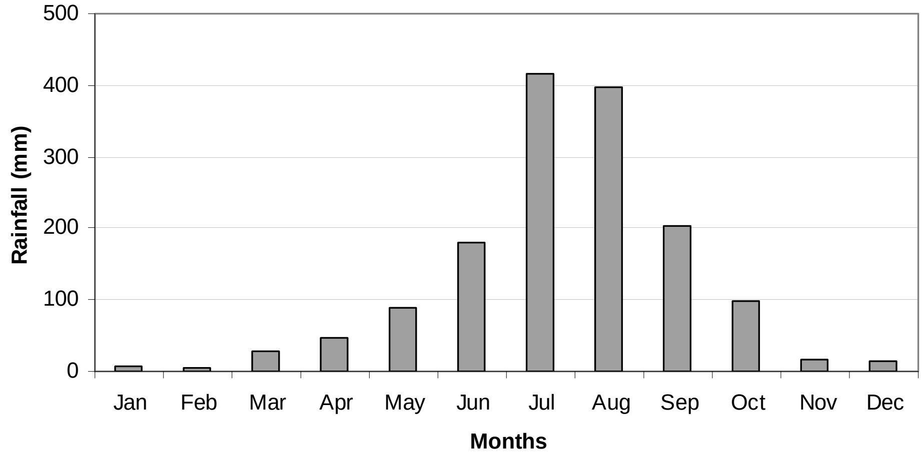

Figure 2-6: Distribution of monthly Rainfall (1997-2007)

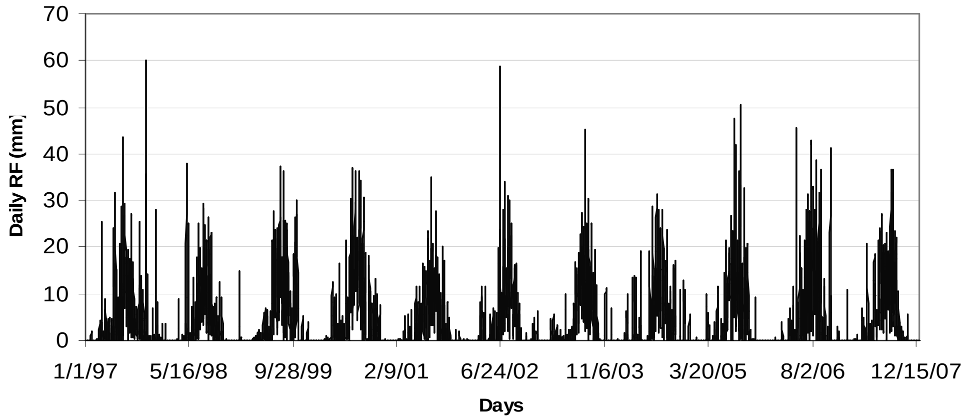

Figure 2-7: Distribution of Daily Rainfall (1997-2007)

2.5. Temperature

Figure (2-8) shows the maximum and minimum monthly temperature calculated using the long term daily record of Debre Tabor station. Accordingly, the hottest month is March with maximum daily temperature of 25 ^{o}C and minimum temperature of 11 ^{o}C, the coldest month is July with maximum temperature of 19^{o}C and minimum temperature of 11^{o}C.

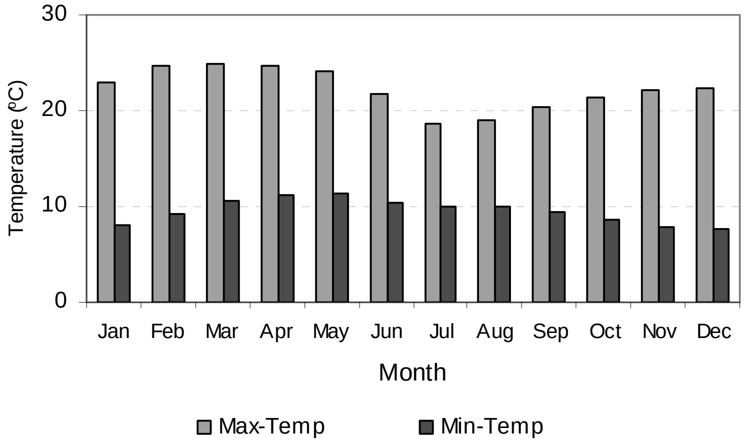

Figure 2-8: Distribution of maximum and minimum monthly temperature

2.6. Hydrological Data

Hydrological data is available from the Ribb river hydrometric station at 12.00^{o} North, 37.72^{o} East that is operational since 1959. The nearest town to the gauging site is Addis Zemen. At the gauging site high flows are recorded during the wet season.

The relevant hydrometric station to estimate river flows at the Ribb dam site is the Upper Ribb near Debre Tabor station, with catchment area of 668 km^2. The station has been operational since 1983.

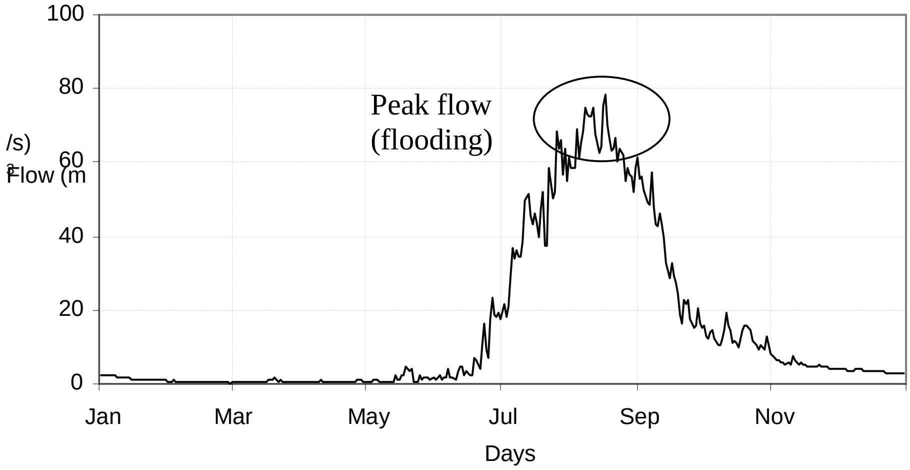

Figure 2-9: Ribb river flow near Addis Zemen

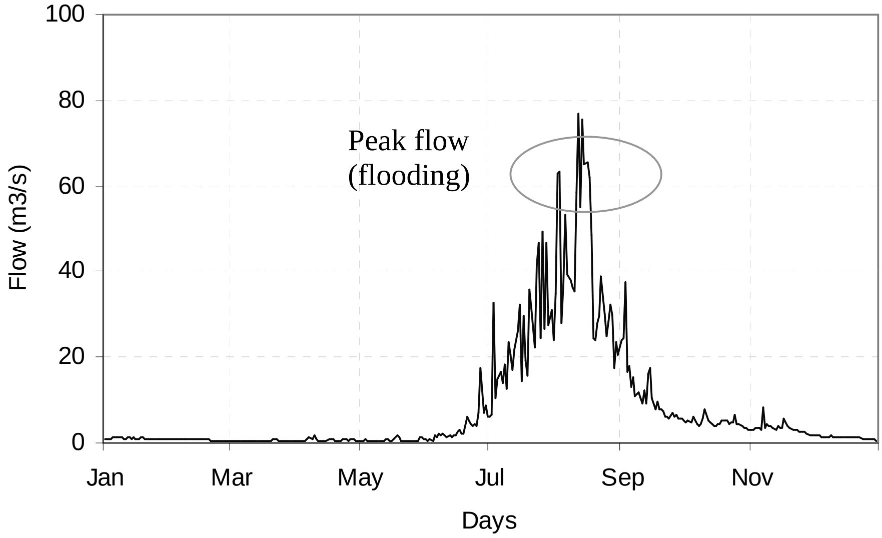

Figure 2-10: Ribb river flow at reservoir site

2.7. Evapotranspiration

The mean annual evapotranspiration of the study area calculated based on ten years data (1997 and 2006) of the two nearby weather stations (Debre Tabor and Gondar) using Penman-Monteith method amounts to 1304 mm and is less than the mean annual precipitation of 1613 mm. As shown in Figure 2-11 the amount of reference evapotranspiration increases almost linearly from September and reaches at its maximum value in March then declines to a minimum value in July.

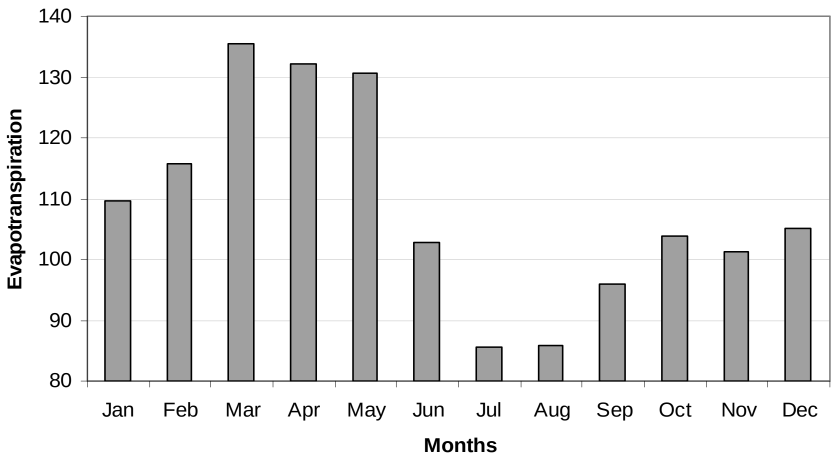

Figure 2-11: Mean monthly evapotranspiration

2.8. Vegetation and Landcover

The reservoir site area is characterized by scars and scattered remnants of trees that are confined along old cultivated terrace lands, streams and riverbanks. The reservoir site area is extensively used for farming, settlements being denser at the upper reservoir slopes and top of the hills. Most of the catchment area is characterised by cropland with scarce eucalyptus poles and few areas of highland area covered by forests.

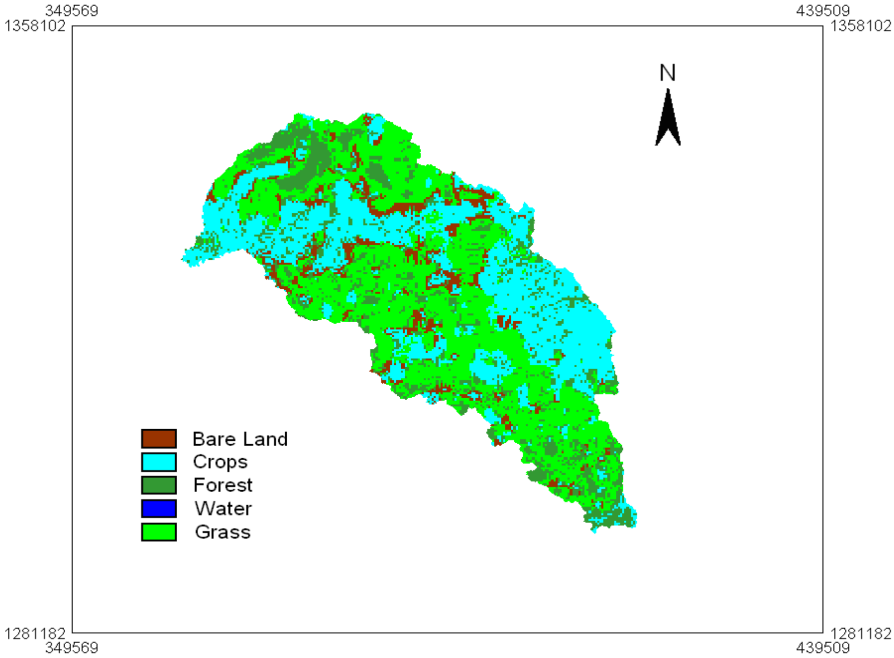

Figure 2-12: Land cover map of Ribb catchment

2.9. Geology

The geology of the Ribb basin is dominated by a huge volcano named Guna Terara. It corresponds to the eruptive events that have occurred during the early Miocene to Pliocene periods, and is classified in the shield group basalt. The common lithotype for this material refers to lenticular basalt with large amount of interbeded scoriaceous lava and basalt agglomerates. Some paleosoils may be interbeded.

The other smaller volcanoes located at the north are also considered being active during the same geological period. The lower part of the valley before Lake Tana is completely overlain by recent fluvial depositions, which are mainly formed by silt to clay deposits. Recent volcanic flows have also been noted but they appear to be localized in the lower section of the Ribb plain. No evidence of such flows has been mapped in the upper parts of the Ribb basin.
There is no evidence of slope instability in the Ribb Reservoir. This is mainly due to the smooth landscape of the reservoir. The reservoir might be fairly watertight due to the clayey blanket covering the slopes and to the basaltic agglomerates and the tuffs formations series forming the reservoir.

3. Reservoir Water Balance

3.1. Introduction

The reservoir water balance computation was made on the basis of water accounting principle by considering all waters inflow, outflow and change in storage of the reservoir. This principle is described schematically in Figure 3.1.

The inflow components are:

- Runoff from the catchment area (R)
- Precipitation on the reservoir area (P) and
- Groundwater inflow to the reservoir (G_{in}).

The outflow components are:

- Water supply from the reservoir (Q_{out}),
- Evaporation from the reservoir (E) and
- Groundwater outflow (G_{out}).

Change in storage (ΔS) is the remaining component which is the difference between all inflow and outflow from the reservoir.

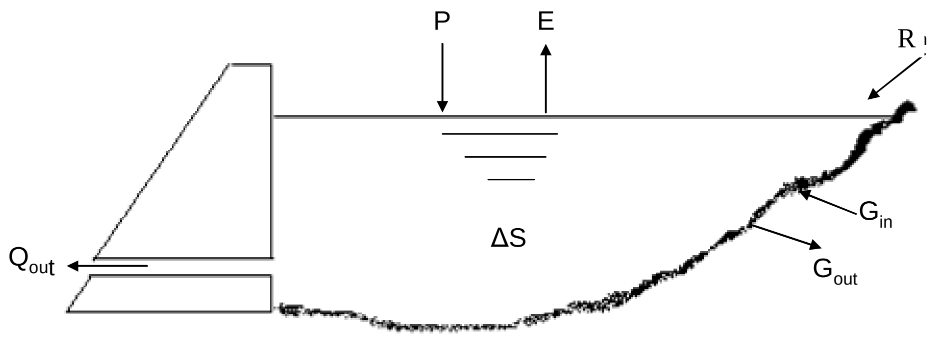

Figure 3-1: Schematic representation of the reservoir water balance components

3.2. Data

The data used for this study includes satellite images (Aster) and data collected during field campaign from Addis Ababa meteorological agency, Ministry of Water Resources, and meteorological office Bahirdar branch. The field campaign was held in September at the end of rainy season in the area. Table 3-1 shows data collected for the area.

Table 3-1: Weather data

Station name	Location		Weather parameters	Temporal resolution
	Lat	Long		
Debre Tabor	11.85	38.01	Precipitation, maximum and minimum temperatures, wind speed, sunshine hour and relative humidity	Daily
Addis Zemen	12.12	37.87	Precipitation, maximum and minimum temperatures	Daily
Gondar	12.55	37.42	Precipitation, maximum and minimum temperatures, wind speed, sunshine hour and relative humidity	Daily

3.3. Water Balance Analysis

3.3.1. Reservoir Water Balance Equation

In general the reservoir water balance equation is:

$$\Delta S = P + R + G_{in} - E - Q_{out} - G_{out} \qquad 3\text{-}1$$

Where,

ΔS = Change in the reservoir water storage
P = Precipitation on the reservoir
R = Runoff into reservoir
E = Evaporation from reservoir
G_{in} = Groundwater inflow
G_{out} = Groundwater outflow
Q_{out} = Outflow

Ribb reservoir has to serve as a storage reservoir and such reservoirs are usually constructed either on formations which are characterized with lesser seepage or on a foundation treated to keep the seepage to a minimum. Owing to this fact the groundwater inflow and outflow components were considered negligible and are not considered in the reservoir water balance equation. Equation 3.1 is subsequently reduced and rearranged to:

$$\Delta S = P + R - E - Q_{out} \qquad 3\text{-}2$$

3.3.2. Water Balance Components Derivation

3.3.2.1. Outflow, Change in Storage and Rainfall

Outflow, and change in storage were derived by using the amount of water needed for irrigation and environmental flow for environment protection. The rainfall data recorded at Debre Tabor and Addis Zemen, was taken for this study as they are the nearest stations to the reservoir.

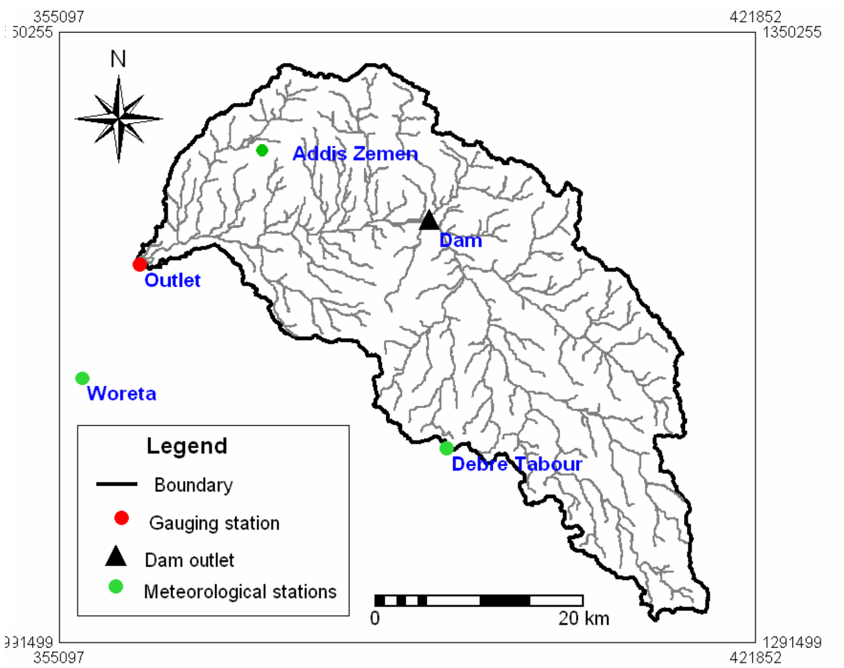

Figure 3-2: Locations of weather stations

3.3.2.2. Evaporation

Evaporation occurs when liquid water changes phase to become water vapour. For the calculation of evaporation from open water surface there are various methods.. Energy balance approaches and mass transfer approaches are include different versions of these methods. The mass transfer approach gives the instantaneous rates of evaporation under given instantaneous values of wind speed and vapour pressure. (Dingman, 1994).

The energy balance approach to determining the average rate of evaporation over time a period Δt and involves measuring or otherwise determining the rate of energy input and output by various modes, along with the change of energy stored in the water body during Δt (Dingman, 1994). The applicability of this approach is limited because it requires measurement of water surface temperature.

The most advanced resistance-based model of evaporation used in hydrologic practice is Penman–Monteith equation, it assumes that all the energy available for evaporation is accessible by the plant canopy, and water vapour diffuses first out of the leaves against the surface (or stomatal) resistance r_s and then into the atmosphere above against the aerodynamic resistance. Meanwhile, the sensible heat, which is originated outside rather than inside the leaves, only has to diffuse upward against the aerodynamic resistance ra. Solving the equations describing the diffusion process produces Penman-Monteith equation (Maidment, 1993). This equation allows the calculation of evaporation from meteorological variables and resistances, which are related to the stomatal and aerodynamic characteristics of the crop.

$$ET_o = \frac{0.408\,\Delta(R_n - G) + \gamma\left(\frac{900}{T} + 273\right)U_2(e_s - e_a)}{\Delta + \gamma(1 + 0.34U_2)} \qquad 3\text{-}3$$

Where, ET_o is evapotranspiration, R_n is the net radiation, G is the soil heat flux, (e_s - e_a) represents the vapour pressure deficit of the air, U_2 is wind speed at 2m height, Δ is the slope of the saturated vapour pressure curve (kPa^{0}C^{-1}) formulated as:

$$\Delta = \frac{4098\,e_s}{(237.3 + Ta)^2} \qquad 3\text{-}4$$

Where, e_s is the average daily saturated vapour pressure (kPa) at average daily temperature *Ta* in (^{0}C).

The psychrometric constant γ (KPa^{0}C^{-1}) is given as:

$$\gamma = 0.0016286\frac{P}{\lambda} \qquad 3\text{-}5$$

Where, *P* = Average barometric pressure (kPa)

λ = the latent heat of vaporization (MJkg^{-1}).

The relative humidity RH and saturated vapour pressure e_s are given in Equations 3-6 and 3-7 respectively:

$$RH = \frac{e_s}{e_a} \times 100 \qquad 3\text{-}6$$

$$e_s = 0.6108\ \exp\left[\frac{17.27\,Ta}{237.3 + Ta}\right] \qquad 3\text{-}7$$

3.3.2.3. Penman open Water Evaporation

Since potential evaporation occurs from an extensive open water surface, it follows that $r_s = 0$ is the appropriate value of surface resistance for estimating potential evaporation. Penman open water evaporation equation or a combination equation is special case of Penman–Monteith equation. Over extensive water surface r_s is taken to be zero and r_a is empirically determined by Penman (1948) is:

$$r_a = \frac{4.72\left[\ln\left(\frac{Z_2}{Z_0}\right)\right]^2}{1 + 0.536 U_2} \tag{3-8}$$

Where, z_2(m) is the height at which meteorological variables are measured, and z_o (m) is the aerodynamic roughness of the surface.

For standardized measurement height of 2 m for wind speed, temperature and humidity adopting a z_o = 0.00137 m which, according to Thom and Oliver (1976) implicitly assumed by Penman (1948) the final equation reads (Maidment, 1993):

$$E = \frac{\Delta}{\Delta + \gamma}(R_n + A_h) + \frac{\gamma}{\Delta + \gamma}\frac{6.43(1 + 0.536 U_2)D}{\lambda} \tag{3-9}$$

Where

E = Open water evaporation

R_n = net radiation exchange for the free water surface, mmday^{-1}

A_h = energy advected to the water body, mm day^{-1}

U_2 = wind speed measured at 2m, ms^{-1}

D = vapour pressure deficit e_s-e_a, kPa

Δ = slope of saturated vapour pressure, kPa^{0}C^{-1}

γ = psycrometric constant, kPa^{0}C^{-1}

λ = latent heat of vapourization, MJkg^{-1}

The magnitude of advection and heat storage effects depends in large on the area, volume and residence time of water in the reservoir relative to the time period of the analysis (Dingman, 1994).

In summer time the water stored in the reservoir is almost completely used and for this reason the effect of advection and heat storage is considered insignificant and is taken to be zero.

The equation of evaporation for the reservoir is therefore reduced to:

$$E = \frac{\Delta}{\Delta + \gamma}R_n + \frac{\gamma}{\Delta + \gamma}\frac{6.43(1 + 0.536U_2)D}{\lambda} \tag{3-10}$$

The net radiation has been calculated according to the procedures and the equations in FAO Irrigation and Drainage Paper No. 56 (Allen et al., 1998).

The input weather data were taken from the nearest stations to the reservoir (Debre Tabor and Addis Zemen). Addis Zemen station has only maximum and minimum temperatures, these are however not sufficient to apply Penman's equation. The remaining required weather parameters were therefore taken from Gondar, which is the next nearest station to the reservoir.

3.3.2.4. Rainfall

Rainfall in the catchment is a large component of inflow in the wet season. The amount of rainfall in the catchment is estimated by using Thiessen polygon and inverse distance methods.

I. Thiessen Polygon Weighting Method

The first method of mean areal precipitation computation is by the Thiessen polygon method. In the Thiessen polygon method, the upstream area of the reservoir is divided into polygons with the rain gauge in the centroid of each polygon assumed to be representative for the rainfall on the area in the polygon. After defining the number of polygons and their respective areas (A_i), then we can determine the weight as ($W_i = A_i/A$) and the areal rainfall is computed as:

$$\overline{P} = \frac{1}{A}\sum_{i=1}^{i=n} A_i \times P_i \qquad 3\text{-}12$$

Where,

$\overline{P}$ = Average rainfall

P_i = Rainfall measured at stations,

A_i = Area of subregions and

A = Total area of the reservoir.

II. Inverse Distance Weighting Method

The Inverse Distance Weighting method is an alternative to the Thiessen polygon weighting method in which a precipitation value at unknown point P(x,y) is interpolated into the centre of the catchment by using the inverse distance squared between the point location and the gauge location as a weight for each gauge.

$$\overline{P} = \frac{d_i^{\frac{1}{m}}}{\sum_{i=1}^{n} d_i^{\frac{1}{m}}} \times P_i \qquad 3\text{-}13$$

Where,

$\overline{P}$ = Estimated average rainfall

P_i = Rainfall measured at stations

d_i = Distance of station from the reservoir centre

m = Weight

n = Number of meteorological stations.

3.3.2.5. Surface Water Inflow

Surface water inflow to the reservoir includes water by rivers, streams and direct overland flow. The main inflow to the reservoir is Ribb river and dominates the surface water inflow. The continuous daily flow data recorded in the reservoir outlet is used for the simulation of water balance and related reservoir capacity.

3.3.3. Computation of Reservoir Capacity

The reservoir capacity is the amount of water a surface reservoir is capable of storing. Yield, demand and storage analysis can be used to determine the volume of water that should be stored in order to provide a specified water demand. Design storage depends on the volume of demand and the hydrology of the catchment supplying the reservoir. The effect of hydrology of the catchment on the required storage volume depends on the temporal uniformity, or lack of it, of the stream flow and the casual rainfall.

The catchment yield or reservoir yield (inflow to the reservoir) and the outflow from the reservoir are the only two factors, which govern the storage capacity of the reservoir. Since the inflow to the reservoir is variable, water is stored in the reservoir to cater to the required outflow from the reservoir, particularly during the critical periods in non-monsoon season. After assessing the monthly or annual inflow of the reservoir the demand pattern can be specified. The reservoir is then usually designed to meet the specified outflow demands (Vijay and Sasikumar, 2003).

The reservoir capacity, the reservoir yield, and the outflow from the reservoir are governed by the storage equation 3-14, given by:

$$\textbf{Change in storage = inflow – outflow} \tag{3-14}$$

3.3.4. Data Requirement

In order to estimate the amount of water to store and supply at the later stage, the down stream water requirement of every month is to be calculated. Similarly, the inflow to the reservoir from the catchment is to be estimated. This analysis will give the optimal water storage requirement so that the down stream area gets water through out the year.

Once the demand and inflow are estimated then it is necessary to need actual demands in appropriate place by geographic and economic criteria. The area-volume curve technique was used to evaluate the reservoir storage.

Procedures for identifying the storage requirement

- Construct a table of inflow (Q_{in}) and outflow (Q_{out})
- Obtain the difference ($Q_{in} - Q_{out}$) for the selected period.
- Obtain the cumulative deficit

Storage = Obtain the cumulative deficit

3.3.5. Area Volume Calculation

The reservoir capacity of the volume of storage, corresponding to a given water level in the reservoir may be calculated either a trapezoidal formula or a prismoidal formula. Thus, if V is the storage volume and h is the contour interval, the formulae by Vijay and Sasikumar (2003) are:

$$V = \sum \frac{h}{2}\left(A_1 + A_2\right)\ldots\ldots \text{(Trapezoidal)}$$

$$= \frac{h}{2}\left\{A_1 + A_n + 2\left(A_2 + A_3 + \ldots\ldots + A_{n-1}\right)\right\} \qquad 3\text{-}15$$

$$V = \sum \frac{h}{3}\left(A_1 + 4A_2 + A_3\right)\ldots\ldots \text{(Prismoidal)}$$

$$= \frac{h}{3}\left[\left(A_1 + A_n\right) + 4\left(A_2 + A_4 + \ldots\ldots\right) + 2\left(A_3 + A_5 + \ldots.\right)\right] \qquad 3\text{-}16$$

Where A_n is the area of the contour corresponding to the water surface elevation in the proposed reservoir. By using the above methods for calculating storage capacity of reservoir, the average volume is derived.

Natural processes like erosion in the catchment area and its deposition in various parts of reservoir gradually reduce the capacity of reservoir. Dead as well as live storages are affected by it. Information about the reduction in capacity is necessary for all the planning and operational purpose that can be obtained through capacity surveys done at regular interval.

The capacity of reservoirs is gradually reducing due to silting and hence sedimentation of reservoir is of great concern to all the water resources development projects. Silting not only occurs in the dead storage but also encroaches into live storage capacity, which has long and short-range impact on the functioning of the project and economics. Correct assessment of the sedimentation rate is essential for assessing useful life of the reservoir as well as optimum reservoir operation schedule.

3.4. HBV Model

3.4.1. Background

The HBV-96 model was originally developed by SMHI in the early 70´s to assist hydropower operations. The aim was to create a conceptual hydrological model with reasonable demands on computer facilities and calibration data. The HBV-96 approach has proved flexible and robust in solving water resource problems and applications now span over a broad range. Furthermore, operational or scientific applications of the HBV-96 model have been reported from more than 50 countries around the world.

The HBV-96 model is today an Integrated Hydrological Modelling System: a modern, well-tested and operational tool. It can be linked with Real Time Weather Information and Forecasting Systems, such as the WebHyPro system developed by SMHI.

The HBV-96 model is a conceptual hydrological model for continuous calculation of runoff. It was originally developed at the Swedish Meteorological and Hydrological Institute (SMHI) in the early 70´s to assist hydropower operations (Bergström and Graham, 1998) by providing hydrological forecasts. The aim was to create a conceptual hydrological model with reasonable demands on computer facilities and calibration data. The model was named after the abbreviation of Hydrologiska Byråns Vattenbalans-avdelning (Hydrological Bureau Waterbalance-section). This was at the time the section at SMHI, where the model was developed. The first operational forecasts were carried out for basins in the northern part of Sweden in 1975.

The basic modelling philosophy behind the model is

- the model shall be based on a sound scientific foundation
- data demands must be met in typical basins
- the model complexity must be justified by model performance
- the model must be properly validated
- the model must be understandable by users.

For the first two decades, only minor changes in the basic model structure were made. In the beginning of the 1990s a comprehensive re-evaluation of the HBV-96 model routines was carried out (Lindström et al., 1997). The model consists of subroutines for snow accumulation and melt, soil moisture accounting, runoff generation and finally, a simple routing river flow.

3.4.2. Structure of the Model

The HBV-96 model can best be described as a semi-distributed conceptual model. Over the years only minor changes in the basic model structure have been made. Input data have been kept as simple as possible, normally only daily mean-values of temperature and precipitation are used. Despite its simplicity, its simulation performance is commendable, and the original use for hydrological forecasting has expanded to applications such as filling gaps in measured time series, simulation of stream-flow in ungauged rivers, design flood calculations and water quality studies input data. The flexible structure of the HBV-96/IHMS system allows the model to make necessary sub-divisions with respect to different climate zones, land-use, and density of the hydrometeorological network. Figure 3-3 gives the schematic diagram of the HBV-96 model structure (SMHI, 2006).

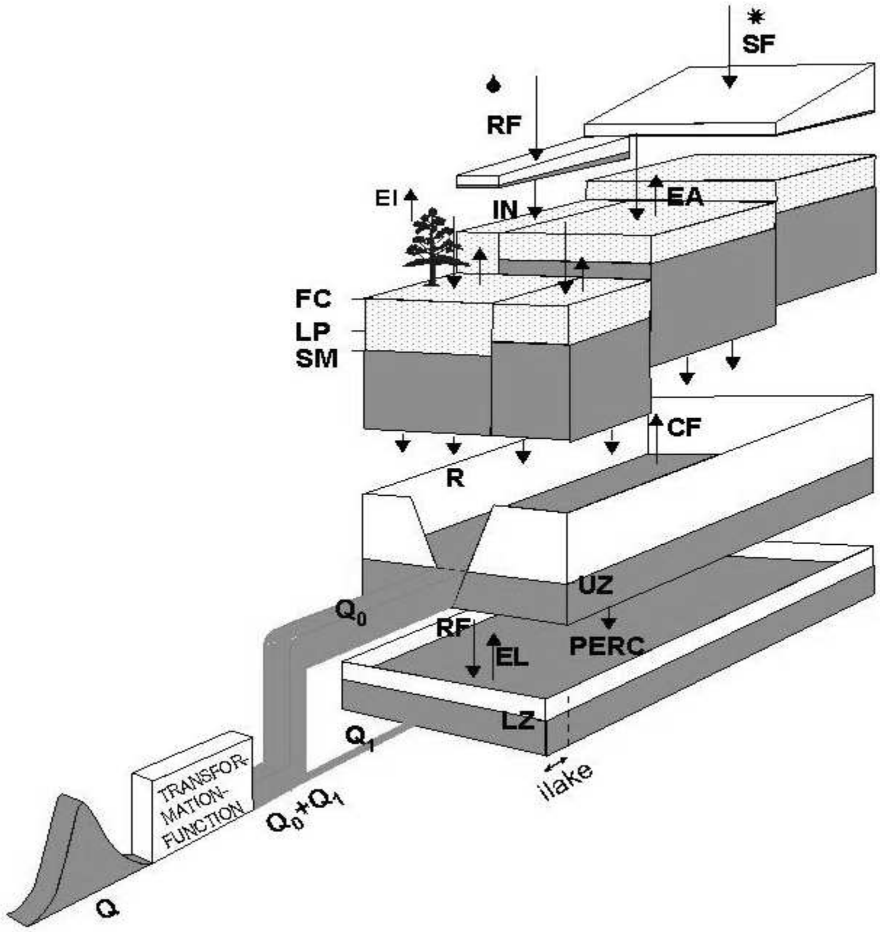

Figure 3-3: Schematic representation of the HBV-96 model.

The general water balance equation used in HBV-96:

$$P - E - Q = \frac{d}{dt}\left[SP + SM + UZ + LZ + Lakes\right] \qquad 3\text{-}17$$

Where,

P = Precipitation (mm)
E = Evapotranspiration (mm)
Q = Runoff (m^3/s)
SP = Snow pack (mm)
SM = Soil moisture (mm)
UZ = Upper groundwater zone (mm)
LZ = Lower groundwater zone (mm)
$LAKES$ = Lake volume (m^3)

3.4.3. Model Routine

Precipitation and Snow Accumulation

Precipitation calculations are made separately for each elevation/vegetation zone within a subbasin. There is separate rainfall and snowfall correction factors as observed precipitation values often are affected by observation losses. The largest errors are related to wind effects and are generally higher for snow than for rain. The general precipitation correction factor accounts for systematic errors that may be caused by non-representative precipitation input. It is possible to use different snowfall correction factors for forested and non-forested zones within a sub-basin.

Soil Moisture

The soil moisture accounting routine is the main part of controlling runoff formation. This routine is based on the three parameters, *β*, *lp* and *fc*:

- *β* controls the contribution to the response function (ΔQ/ΔP) or the increase in soil moisture storage (1-ΔQ/ΔP) from each millimeter of rainfall or snow melt. The ratio ΔQ /ΔP is often called runoff coefficient, and ΔQ is often called effective precipitation.
- *lp* is a soil moisture value above which evapotranspiration reaches its potential value. The parameter *lp* is given as a fraction of *fc*.
- *fc* is the maximum soil moisture storage (in mm) in the model.

$$\frac{\Delta Q}{\Delta P} = \left(\frac{SM}{FC}\right)^{\beta eta} \quad (3\text{-}18)$$

Where,

SM	= Computed soil moisture storage
ΔP	= Contribution from rainfall
ΔQ	= Contribution to the response function
FC	= Maximum soil moisture storage
β	= Empirical coefficient
ET_{pot}	= Eotential evapotranspiration
ET_a	= Computed actual evapotranspiration
LP	= Limit for potential evapotranspiration

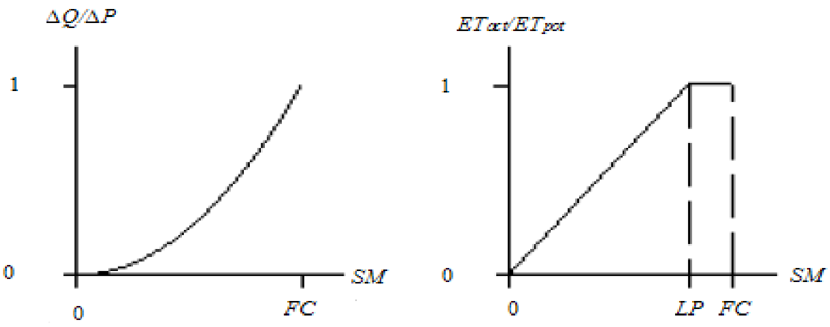

Figure 3-4: The soil moisture routine

The effect of the soil routine is that the contribution to runoff from rain or snow melt is small when the soil is dry (low soil moisture values), and great at wet conditions. The actual evapotranspiration decreases as the soil dries out. Long-term mean values are used as estimates of the potential evaporation at a certain time of the year. It is thus assumed that the interannual variation in actual evapotranspiration is much more dependent on the soil moisture conditions than on the interannual variation in potential evaporation.

Response Routine

The runoff generation routine is the response function which transforms excess water from the soil moisture zone to runoff. This routine consists of one non linear upper reservoir in the upper zone and one linear reservoir in the lower zone. These two reservoirs are the origin of the quick and slow runoff component of the hydrograph. The outflow from the upper reservoir is described by function corresponding to a continuously increasing recession coefficient

$$Q_o = K * UZ^{(1+alfa)} \qquad \text{3-19}$$

Where, Q_0 = outflow from upper reservoir (mm)

$Alfa$ = a measure of the non linearity and has a value range from 0.5 to 1.1

UZ = the upper reservoir content (mm)

K = the recession coefficient, parameters used in computing for the value of K are Khq, Hq and $Alfa$.

Hq = high flow level

Khq = recession rate

$$Hq = \frac{86.4\sqrt{Mq * Mhq}}{A} \qquad \text{3-20}$$

Where, Mq = the mean of the observed discharge (m^3/s)

Mhq = the mean of annual peaks (m^3/s)

A = the catchment area (km^2)

$$Q_1 = K_4 * LZ \tag{3-21}$$

Where, Q_1 = yield from the lower reservoir (mm)
LZ = the lower reservoir content (mm)
K_4 = the recession coefficient

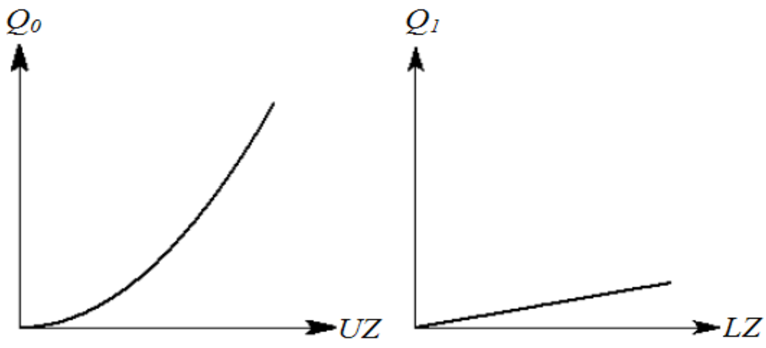

Figure 3-5: The response routine

Transformation Function

The runoff generated from the response routine is routed through a transformation function in order to get a smooth of the hydrograph at the outlet of the subbasin. The transformation function is a simple filter technique with a triangular distribution of the weights, as shown in Figure 3-6. The time base of the triangular distribution is given by the parameter *maxbaz*. *Maxbaz* is the new parameter for the transformation function and shall be used in all new calibrations since it is independent of the time-step.

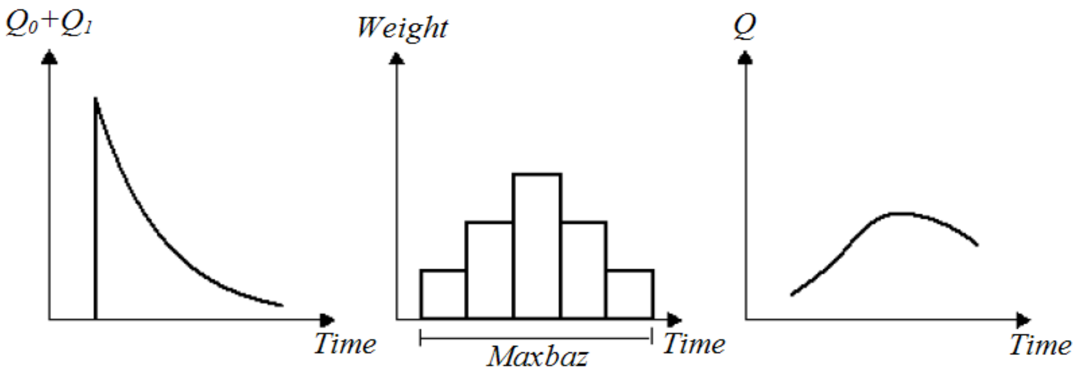

Figure 3-6: The transformation function

3.4.4. Model Calibration

Hydrological models require adjustment of the values of model parameters, hydrologic influence and stresses in order to tune the model. By model calibration that stands for the fine-tuning of the input parameter data, the performance of the model will improve. The procedure of adjusting the model input parameters is necessary to mach with model output with measured field data for the selected period and situation entered to the model (Rientjes, 2007).

The three methods of assessing the fitness of the calculated and recorded runoff are:

- By visual interpretation of the hydrograph
- By relative volume error
- By Nash and Sutcliffe efficiency

The relative volume error is given by equation 3-22

$$R = \frac{\sum_{i=1}^{n} Q_{sim(i)} - \sum_{i=1}^{n} Q_{obs(i)}}{\sum_{i=1}^{n} Q_{obs(i)}} \times 100\% \qquad \text{3-22}$$

Where $Q_{obs(i)}$ = observed discharge at time $_i$
$Q_{sim(i)}$ =simulated discharge at time $_i$

and the Nash-Sutcliffe model efficiency coefficient (Nash and Sutcliffe, 1970) is given by the Equation 3-23,

$$R^2 = 1 - \frac{\sum_{i=1}^{n} \left[Q_{sim}(i) - Q_{obs}(i)\right]^2}{\sum_{i=1}^{n} \left[Q_{obs}(i) - \overline{Q_{obs}}\right]^2} \qquad \text{3-23}$$

Where; Q_{sim} = Simulated discharge
Q_{obs} = Observed discharge

3.4.5. Setup of the Model

The HBV-96 model uses daily meteorological and hydrological data. Rainfall, evapotranspiration, temperature and forest and non forest landcover data are the inputs of the model. Elevation data used for this work is taken from ASTER DEM and for calibration and validation discharge data is needed. Penman-Monteith method is used for evapotranspiration estimation.

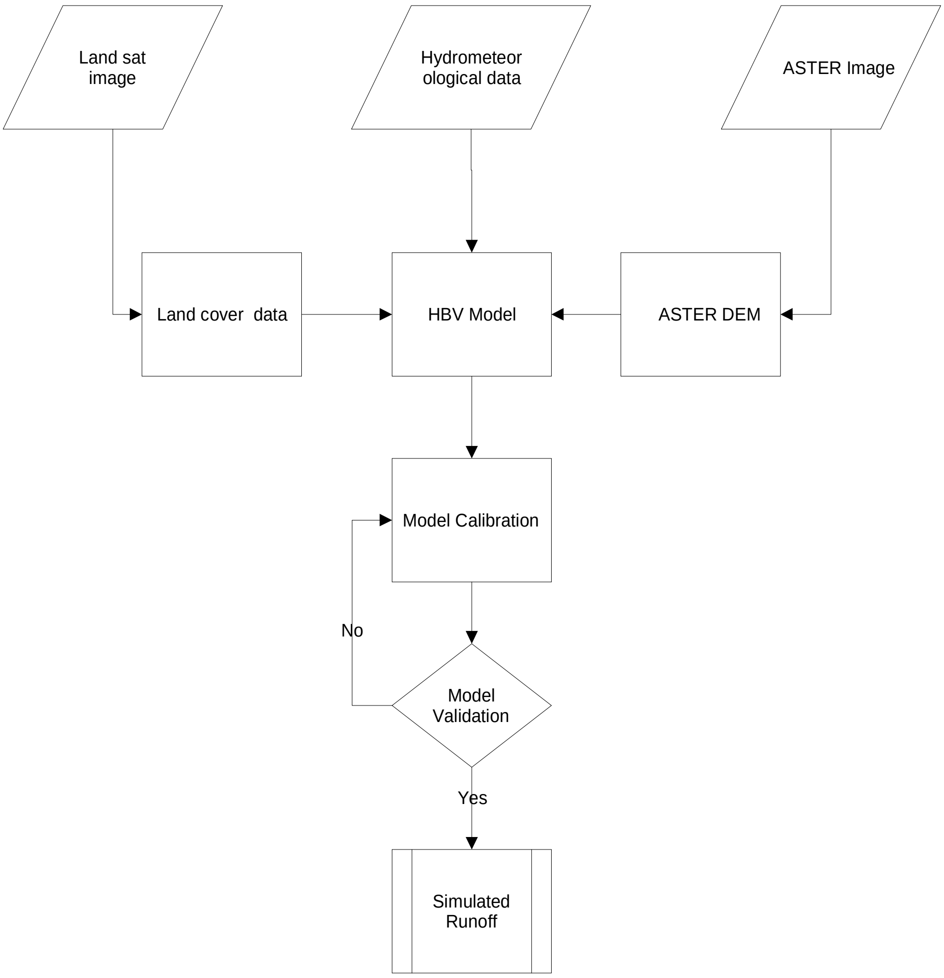

Figure 3-7: The flow chart of the HBV-96 model setup

The size of the study area is 668 square kilometres. Figure 3-8 gives the three subbasins of the catchment and the percentage of landover for each subbasin is given in Table 3-2. Land cover map is obtained from Landsat image and has different groups of landcover and in this study the HBV-96 model uses only forest and non-forest types for this study and the original map was resampled to fit the model.

Table 3-2: The three subbasins area:

Subbasin Name	Area (km^2)
Subbasin1	238.45
Subbasin2	210.97
Subbasin3	259.49
Total basin area 668 km^2	

Figure 3-8: Upper Ribb catchment divided into three subbasins

The landcover area for the three subbasins is given in Table 3-3. The elevation group is at 100 meter interval for each subbasin.

Table 3-3: Subbasin area and landcover type

Subbasin	Land Cover Name		Total Area (km^2)
	Field (km^2)	Forest (km^2)	
Subbasin-1	190.40	48.04	238.45
Subbasin-2	185.05	25.91	210.97
Subbasin-3	227.25	32.23	259.49

For rainfall estimation the inverse distance method was used. The weights of the two rainfall stations are given in Table 3-4.

Table 3-4: The two station weights

Station Name	Subbasin-1	Subbasin-2	Subbasin-3
Debre Tabor	0.88	0.9	0.73
Addis Zemen	0.12	0.1	0.27

Data used for this study was from 1997-2006 out of these data from 1997-2001 for calibration and from 2003-2006 for validation. Usually, a 10-year daily time series data is used in calibrating and validating HBV-96 model (Lindström et al., 1997). Table 3-5 shows a list of sensitive parameters used in HBV-96 calibration.

Table 3-5: Parameters used for calibration

Model Routine	**Parameter**	**Description**
Soil moisture	*FC*	Maximum soil moisture storage (mm)
	LP	Limit for potential evaporation (mm)
	Beta	Exponent in the equation for discharge from the soil water zone
Response function	K_4	Recession coefficient for the lower response box
	Khq	Recession coefficient for the lower response box when the discharge is *Hq*
	Hq	Calculated value (m^3/s)
	Alfa	Used in the equation $Q_o = K * UZ^{(Alfa+1)}$

3.5. Irrigation and Crop Water Requirement

According to United Nations Environmental Programme’s (UNEP, 2000) Global Environmental Outlook, freshwater scarcity is viewed by both scientists and politicians as the second most important environmental issue of the 21st century. ‘‘water requirement’’ means the amount of water that must be supplied to the crop by irrigation to achieve optimal crop growth.

Water is often a limiting factor for crop growth, especially in arid and semi-arid regions, but even in some in humid areas. In order to achieve optimal crop productivity, a certain amount of water must be applied to the soil such that evapotranspiration may occur at the potential rate. Only part of the applied water is actually ‘‘used’’ by the plant and evapotranspirates; this amount, the difference between the potential evapotranspiration and the evapotranspiration that would occur without irrigation, is the net irrigation requirement. The other part of the added water serves to leach salts from the field soils, leaks or evaporates unproductively from the irrigation canals, or runs off; this amount depends on irrigation technology and management. The ratio of the net irrigation water requirement and the total amount of water that needs to be withdrawn from the source, the gross irrigation requirement, is called ‘‘irrigation water use efficiency.’’ Under conditions of restricted water availability, farmers may choose to irrigate at a lower than optimal rate. Then the actual water withdrawal is less than the gross irrigation requirement, and, equally, the actual consumptive water use for irrigation is less than the net irrigation requirement (Doll and Siebert, 2002)

An important part of any evaluation of water supply and water requirements, where water is a scarce commodity and seasonally variable, is to match the water supply and water requirement (demand) profiles as closely as possible. For example, cropping patterns and areas occupied by various crops, can be manipulated to accommodate a diminishing water supply towards the end of rainy season. Also, land preparation and dates of planting can be staggered to smooth away peak water demand where it exceeds water supply in certain months (FAO, Soil bulletin 55).

3.5.1. Crop Water Demand

The crop water need, or in other words the amount of water needed by a certain crop to grow optimally, mainly depends on:
Climate: - in sunny and hot climate, crops need more water per day than in a clouded and cool climate.
Crop type: - crops like rice or sugarcane need more water than crops like beans or wheat and Growing stage of the crop: - fully grown crops need more water than crops than have just been planted.

$$ET_m = K_c ET_o \qquad 3\text{-}24$$

Where, ETm = Crop water requirement optimally (mm)
Kc = Crop factors (depends on crop type and development stages)
ETo = Referential evapotranspiration (depends on climatic factors) (mm)

The relation described in the above equation determines major crops water requirement of the study area. Major crops in the study area selected as they are frequently cultivated in the area. The selected crops are maize, rice, Teff, millet and potato. The crop water requirement and the water requirement for irrigation calculated by using CROPWAT for windows as described below.

3.5.2. CROPWAT

CROPWAT is a decision support system developed by the Land and Water Development Division of FAO. Its main functions are:

To calculate:

- Reference evapotranspiration
- Crop water requirements
- Crop irrigation requirements

In order to develop irrigation schedules under various management conditions for scheme water supply and to evaluate rainfed production, drought effects and efficiency of irrigation practices.

CROPWAT is meant as a practical tool to carry out standard calculations for evapotranspiration and crop water uses, and more specifically to design and to manage irrigation schemes. It allows the development of recommendations for improved irrigation practices, the planning of irrigation schedules under varying water supply conditions, and the assessment of production under rainfed

conditions or deficit irrigation. Calculations of crop water requirements and irrigation requirements are carried out with inputs of climatic and crop data (Smith, 1996).
CROPWAT for Windows is a program that uses the FAO (1992) Penman-Monteith methods for calculating reference crop evapotranspiration. These estimates are used in crop water requirements and irrigation scheduling calculations (Clarke et al., 1998).

CROPWAT includes a revised method for estimating reference crop evapotranspiration, adopting the approach of Penman-Monteith. Calculations of crop water requirements and irrigation requirements are carried out with inputs of climatic and crop data. The development of irrigation schedules and evaluation of rainfed and irrigation practices are based on a daily soil-water balance using various options for water supply and irrigation management conditions. Scheme s of water supply are calculated according to the cropping pattern provided. Procedures for calculation of the crop water requirements and irrigation requirements are based on methodologies presented in FAO Irrigation and Drainage Papers No. 24 "Crop water requirements" and No. 33 "Yield response to water".

By using CROPWAT software the amount of water requirement for irrigation is estimated.

3.6. Environmental Water Flow

Assessment of water availability, water use and water stress at the global scale has been the subject of increasingly intensive research over the course of the past 10 years. However, the requirements of aquatic ecosystems for water have not been considered explicitly in such assessments. It is, however, critically important that in global studies a certain volume of water is planned for the maintenance of freshwater ecosystem functions and the services they provide to humans. The total EWR are assumed to consist of ecologically relevant low-flow and high-flow components. Both components are related to river flow variability, and estimated by conceptual rules from the discharge time series simulated by the global hydrology model. The concept of environmental water scarcity is then introduced and analyzed using a water stress indicator, which shows what proportion of the utilisable water in world river basins is currently withdrawn for direct human use and where this use is in conflict with EWR. EWR required to maintain a fair condition of freshwater ecosystems range globally from 20 to 50 percent of the mean annual river flow in a basin(Smakhtin et al., 2004). It is shown that even at estimated modest levels of EWR, parts of the world are already or soon will be classified as environmentally water scarce or environmentally water stressed.

4. Results of Water Balance Components

4.1. Rainfall

The amount of rainfall in the catchment is estimated by using Thiessen polygon and inverse distance methods.

Table 4-1: Thiessen and inverse distance weights of Ribb reservoir

Station	Thiessen polygon Weight	Inverse distance Weight
Debre Tabor	0.664	0.605
Addis Zemen	0.336	0.395

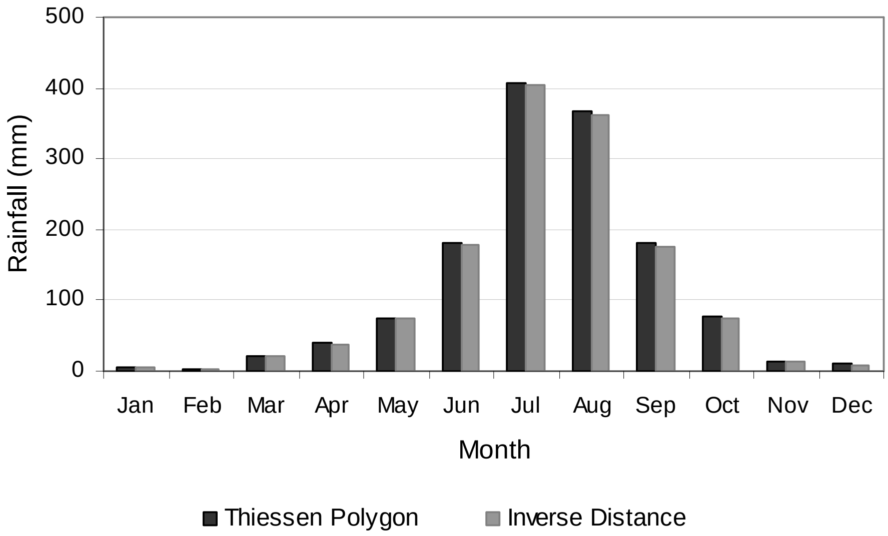

Figure 4-1: Rainfall results of the reservoir by Thiessen polygon and inverse distance weighting.

4.2. Open Water Evaporation

Actual evaporation is a large component of loss of water for the water balance in tropical Africa where Ribb reservoir is located. Actual evaporation rates are difficult to estimate and reliable estimation relies heavily on data availability. Reservoir open water evaporation is estimated using the observed daily meteorological data values at Debre Tabor and Gonder stations. To estimate albedo of the reservoir, if there is no water in the reservoir it is impossible to compute albedo directly, so albedo value of the near by Lake Tana is adopted (Abeyou, 2008) and reservoir evaporation values estimated by Penman combination equation.

Albedo value for Lake Tana ranges from 0.05 to 0.062 with an average of 0.058. An albedo value of 0.058 is used for open water evaporation calculation, this value close to albedo value used at Lake Ziway in Ethiopia which is 0.06 (Vallet-Coulomb et al., 2001). The calculated average value of evaporation on daily basis is 4.7mm/day and a long-term average annual evaporation is 1800mm/year.

In the Figure 4-2 relative humidity, sunshine, temperature and evaporation are drawn to show their relationship.

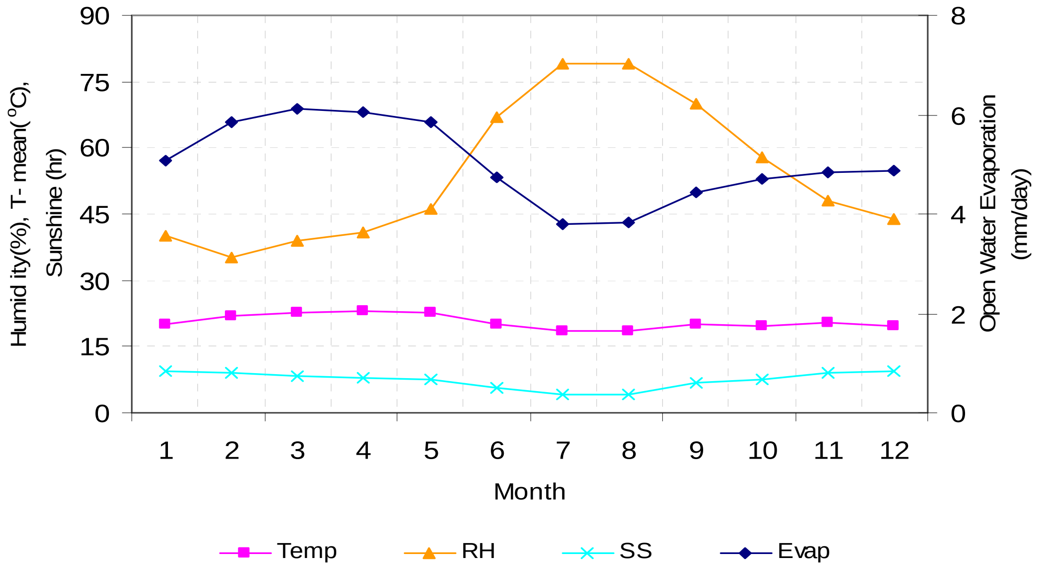

Figure 4-2: The relation of relative humidity, mean temperature, sunshine and evaporation.

4.3. Runoff

The hydrometric station to estimate river flows at the Ribb reservoir site is the Upper Ribb near Debre Tabor station, with upstream catchment area of 668 km^2.

Figures 4-3 and 4-4 show daily stream flow variations at the Upper Ribb gauging station during the rainy season (July-September) for the wet year of 1998, annual flow over the same record was 603 Mm^3. For the dry year of 2004 the flow was 138 Mm^3 that was nearly 41% of the wet year flow. July and August rainfall in 2001 was a value of 629 mm, which was about 60% of the 1998 annual rainfall of 1,059 mm.

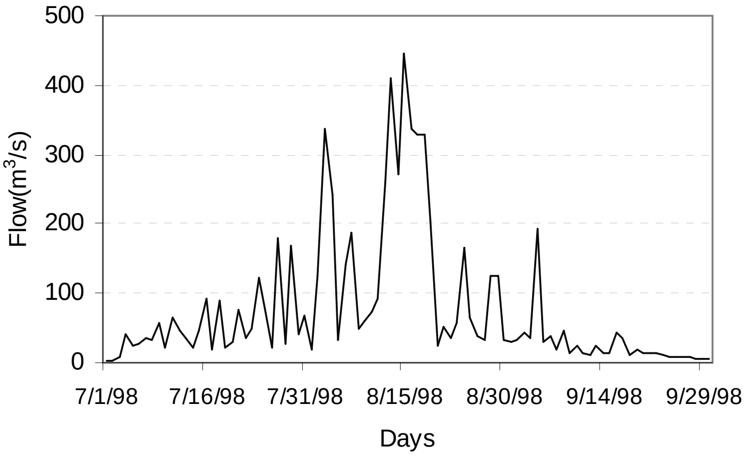

Figure 4-3: Mean daily flow of Upper Ribb (m^3/s) during the wet year of 1998.

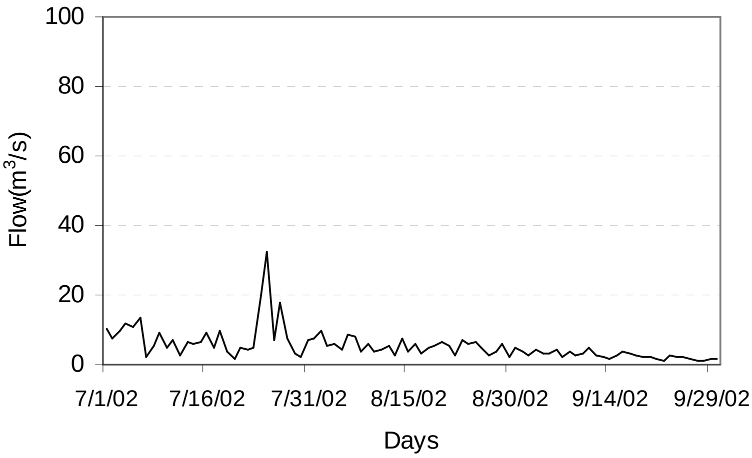

Figure 4-4: Mean daily flow of Upper Ribb (m^3/s) during dry year of 2001.

Runoff time series data are screened for consistency and some unreliable observation records were corrected by hydrologic reasoning. The screened time series data for the catchment is used in the water balance modelling of the reservoir.

Table 4-2: Average annual river flow of upper Ribb

River Name	Area (km^2)	Mean annual river flow (MCM)
Upper Ribb	668	215

4.4. HBV Model

4.4.1. Data Input

The following are input data for HBV-96 model calibration:

- Daily rainfall
- Daily temperature
- Long-term monthly evaporation
- Daily river flow data

The acquired data for this study was divided into three parts. To warm the model one year data is used for initializing the model. Calibration was done for the period 1997-2001 and validation was for the period 2002-2006. Initialization of the model serves to adopt the hydrological model from the modelled environment.

The daily potential evapotranspiration was calculated based on meteorological station located near Ribb reservoir (Debre Tabor, and Gondar stations) using FAO Penman-Monteith equation. Areal distribution of potential evaporation of the reservoir is then estimated using inverse distance square interpolation of the two stations. Table 4-3 shows the weights of stations for the areal potential evapotranspiration and temperature estimation.

Table 4-3: Evapotranspiration weights of meteorological stations on the catchments

Stations	Weight
Debre Tabor	0.9
Gondar	0.1

4.4.2. Model calibration

The calibration of the model is usually done by manual try and error technique (Bergström, 1992). Different criteria can be used to assess the fit of simulated runoff to observed runoff. Calibration is fine-tuning of the selected parameters which have a significant role for model performance. After running the model for different trials the optimum parameter is chosen to match the simulated and the recorded flow. Model performance was evaluated by:

- Visual inspection of plots with Q_{sim} and Q_{obs}
- By Nash and Sutcliffe efficiency criteria
- By relative volume error

The data for calibration was from 1997-2001, Upper Ribb station the outlet of the catchment. The parameters that give the best result are given in Table 4-4. Model performance indicators used are the Nash-Sutcliffe efficiency (R^2) and the relative volume error. The value of the Nash-Sutcliffe efficiency (R^2) is 0.8 for calibration and 0.81 for validation. The relative volume error for validation and calibration is 4% and 3% respectively.

Table 4-4: Parameters used in HBV-96 model

Model Routine Parameter	Parameter	Calibrated value
Soil Moisture	*LP*	0.98
	FC	300
	Beta	2
Response Function	K_4	0.1
	Alfa	1
	Khq	0.2
	Hq	2.6

Nash-Sutcliffe coefficient and relative volume error are the objective functions in HBV-96 model as described below:

The Nash-Sutcliffe Coefficient

The coefficient of efficiency (R^2) is normally used for assessment of simulations by the HBV-96 model and it is given by expression:

$$R^2 = 1 - \frac{\sum_{i=1}^{n}\left[Q_{sim}(i) - Q_{obs}(i)\right]^2}{\sum_{i=1}^{n}\left[Q_{obs}(i) - \overline{Q_{obs}}\right]^2} \qquad 4\text{-}1$$

Where, $Q_{obs(i)}$ = observed discharge
$Q_{sim(i)}$ = simulated discharge at time *i*.
i = time

R^2 compares the prediction by the model with the simplest possible prediction, a constant value of the observed mean value over the entire period.

- $R^2 = 1$, Perfect fit, $Q_{sim(i)} = Q_{obs(i)}$
- $R^2 = 0$, Simulation as good (or poor) as the constant-value prediction
- $R^2 < 0$, Very poor fit

The model performance of HBV-96 model is best from 0.8 to 0.95, in most of the cases above 0.6 values also acceptable (SMHI, 2006).

Relative volume error

The other error is the relative volume error and it is described as by equation 4-2:

$$R = \frac{\sum_{i=1}^{n} Q_{sim(i)} - \sum_{i=1}^{n} Q_{obs(i)}}{\sum_{i=1}^{n} Q_{obs(i)}} \times 100\% \qquad 4\text{-}2$$

Where $Q_{obs(i)}$ = observed discharge at time $_i$
$Q_{sim(i)}$ =simulated discharge at time $_i$

A relative volume error in between ± 5 shows the model performs extremely well, a relative volume error values in between +10% to +5% and -5% to -10% shows a model performs good and a relative volume error greater than $\pm 10\%$ shows the model performance is not good.

Table 4-5: The objective function values obtained during the calibration process

Objective Functions	Value
R^2 (Nash and Sutcliffe)	0.81
Relative volume error	0.04

The discharge hydrograph after calibration is given in Figure 4-5 and 4-6. From these Figures can be seen that the observed and simulated discharge match accurately. The differences are larger in observed and the simulated discharges during the rainy season due to the rain coming from upstream area.

The simulated hydrograph for the dry season matches closely to the observed one. In this case the simulated one is somewhat larger than the observed one. Simulated and observed discharge did not match due to a number of possible reasons. That relates to the selected model approach and available data that is limited in this study. Also high runoff cause that the gauge overtops by flood and the record might not be accurate.

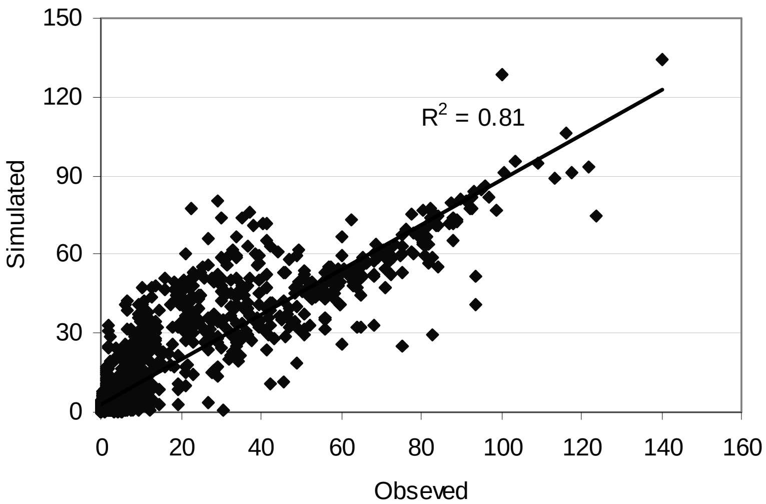

Figure 4-5: Scatter plot of calibration results

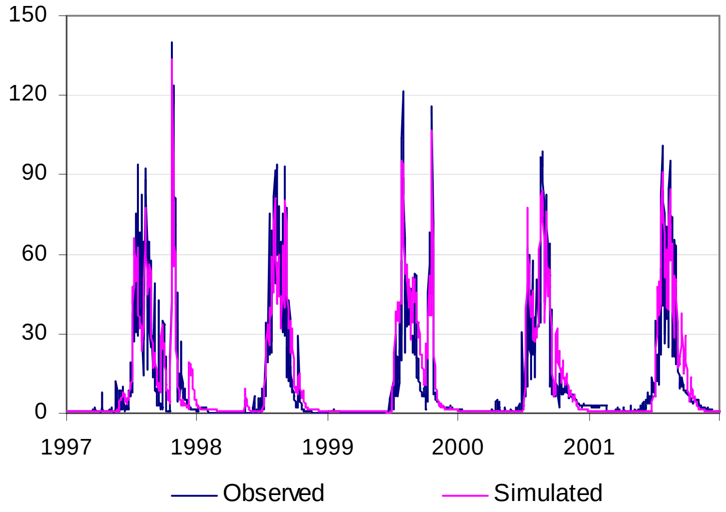

Figure 4-6: Simulated and observed hydrographs after model calibration

4.4.3. HBV Model Validation

Due to the complexity of the real world, representing the real world system by a model approach may not be accurate. Models therefore are uncertain and models cannot be stated reliable when only one field station is simulated. As such, it may occur that under different hydrologic stress conditions the model does not accurately represent the real world system behaviour despite the fact that optimal and calibrated model parameter are used.

Validation is a process of demonstrating that a given site-specific model is capable of making accurate predictions for periods outside a calibration period (Refsgaard and Knudsen, 1996). Simple model structures, calibrated over a certain period, are influenced by the rainfall-runoff sequence specific to that period (Lee et al., 2005) therefore in order to prove validity of a model, the model should be tested against a second, independent set of stress conditions.

Validation was done for the Ribb reservoir catchment with data from 2002 to 2006. The objective functions available in HBV-96 model were used for testing the validity of the modelling on Ribb reservoir. The objective functions used to measure the reliability of the model are the relative volume error and the Nash-Sutcliffe coefficient (R^2).

Table 4-6: The objective function values obtained during the validation process

Objective Functions	Value
R^2 (Nash and Sutcliffe)	0.81
Relative volume error	0.03

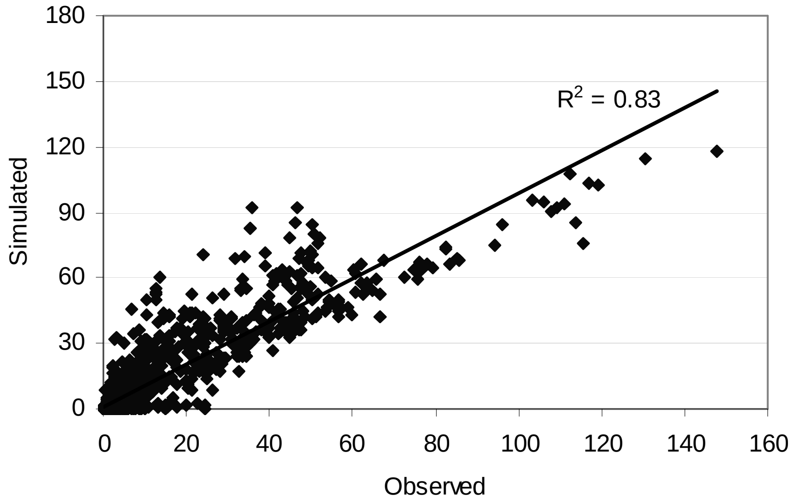

Figure 4-7: Scatter plot of validation results

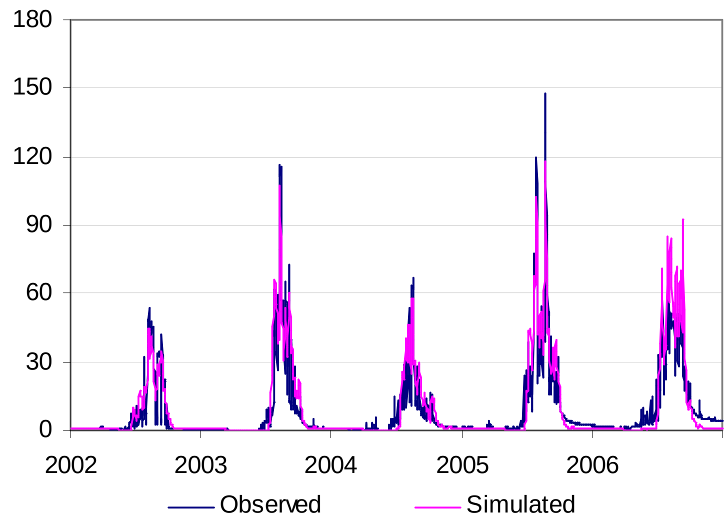

Figure 4-8: Simulated and observed validation result

The performance of the model for validation is similar to the performance of the model in calibration period. As shown in Figure 4-8 above, the hydrograph of the observed base flow is close to the simulated flow. But there is some disagreement between the simulated and the observed in peak flow especially in the year 2006 the simulated peak flows are higher than the observed.

4.5. Storage Capacity

To determine the storage capacity of a reservoir it is important to understand the area of interest with the help of images. The reservoir areas are derived based on the contour lines of the area with digital elevation model of ASTER image.

The Advanced Spaceborne Thermal Emission and Reflection Radiometer (ASTER) is an advanced multispectral imager that was launched on board NASA’s Terra spacecraft in December, 1999 (ERSDAC, 2005). It was placed in a 705 km sun synchronous orbit (at equator) with descending node crossing at about 10:30 am local solar time and the orbital inclination of 98.2 degrees.

The ASTER sensor is designed to provide image data in 14 visible, near-infrared, short wavelength infrared and thermal infrared spectral bands with the spatial resolution of 15m, 30m, 90m separately. Stereo image data are recorded only in Band 3, which is the near-infrared wavelength region from 0.78 to 0.86 μm, using both nadir and aft-looking telescopes.

ASTER has 14 bands from visible to thermal infrared region, which enables to provide more information than that provided by Landsat/TM, ETM+, a representative earth observation sensor. More specifically, Landsat/TM, ETM+ has 2 bands in short wave infrared region (SWIR), whereas ASTER has 6 bands in the region. ASTER data is applicable to define minerals and rocks in resource exploration, environmental monitoring such as vegetation, monitoring of volcanic activity and others. In thermal infrared region (TIR), Landsat/TM, ETM+ has only one band, while ASTER has 5 bands. This is why ASTER is expected to contribute greatly in fields, which require highly accurate temperature and emissivity detection such as identification of ores (felsite from mafic rock), studies on cloud, evapotranspiration, heat island effect in urban areas, monitoring of volcanic activity, heated effluent and others.

Another pronounced feature of ASTER is the capability to collect information, which leads to the production of stereoscopic data by combining them with high spatial resolution spectral information. ASTER band3 in VNIR (0.78-0.86μm) can observe nadir-looking (3N) and backward looking (3B) data simultaneously. Stereoscopic data can be produced by the combination of these data. Also, based on the stereoscopic data, digital elevation model (DEM) can be processed. In this way, ASTER data can add three-dimensional information on topographic map (Baipeng et al., 2007).

The digital elevation model generated from ASTER image is described in Figure 2-3 and the contour lines generated from ASTER image is shown in Figure 4-9. Lines are drawn at five meter interval of contour with reference at the elevation of the outlet of the reservoir at 1850m.

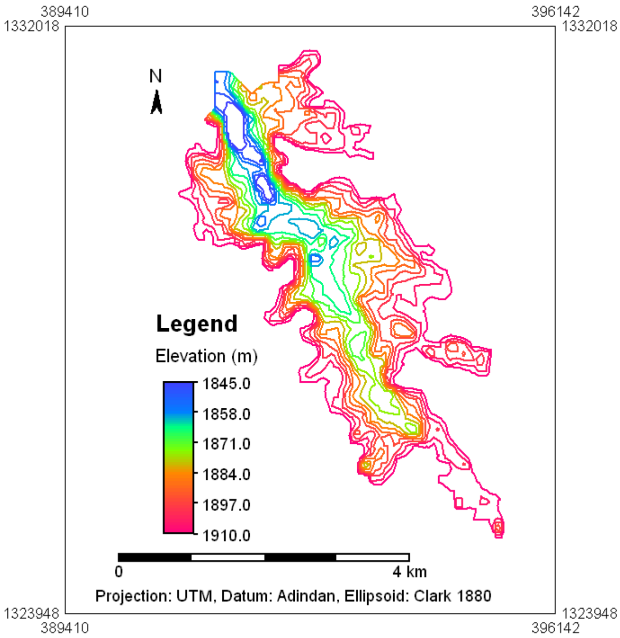

Figure 4-9: Contours generated from ASTER image for the reservoir

The incremental volume between sequential elevation contour lines is determined from the following methods.

- Trapezoidal
- Prismoidal
- ILWIS Script

1. Trapezoidal method

$$= \frac{h}{2}\left\{A_1 + A_n + 2\left(A_2 + A_3 + \ldots.. + A_{n-1}\right)\right\} \qquad 4\text{-}3$$

Where, h = height of contour

A= area of each contour

From the above equation the area of each contour is compiled in Table 4-7
The volume of the reservoir is generated at 5 meters interval of contour in ILWIS software and the volume between successive contour lines are calculated to get the total volume of the reservoir. Results of the trapezoidal method are given in Table 4-7.

Table 4-7: Volume of the reservoir at each elevation by trapezoidal method

Elev.	Area	Volume
1800	0.005	0.00
1805	0.010	0.02
1810	0.014	0.08
1815	0.021	0.17
1820	0.029	0.29
1825	0.037	0.46
1830	0.049	0.67
1835	0.068	0.96
1840	0.096	1.37
1845	0.172	2.04
1850	0.310	3.24
1855	0.476	5.21
1860	0.776	8.34
1865	1.337	13.62
1870	1.890	21.69
1875	2.548	32.78
1880	3.261	47.31
1885	4.063	65.61
1890	4.964	88.18
1895	5.959	115.49
1900	7.090	148.11
1905	8.566	187.25
1910	10.426	234.73

2. Prismoidal method

$$= \frac{h}{3}\left[(A_1 + A_n) + 4(A_2 + A_4 + ...) + 2(A_3 + A_5 + ...)\right] \qquad 4\text{-}4$$

Where, h = height of contour

A= area of each contour

From the above equation the area of each contour is given in Table 4-8

The volume of the reservoir is generated at 5 meters interval of contour in ILWIS software and the volume between successive contour lines estimated to get the total volume of the reservoir. Results of the accumulated values for prismoidal method are given in Table 4-8.

Table 4-8: Volume of the reservoir at each elevation by prismoidal method

Elev.	Area	Volume
1800	0.005	0.00
1805	0.010	0.02
1810	0.014	0.08
1815	0.021	0.17
1820	0.029	0.29
1825	0.037	0.46
1830	0.049	0.67
1835	0.068	0.96
1840	0.096	1.37
1845	0.172	2.04
1850	0.310	3.24
1855	0.476	5.21
1860	0.776	8.34
1865	1.337	13.62
1870	1.890	21.69
1875	2.548	32.78
1880	3.261	47.31
1885	4.063	65.61
1890	4.964	88.18
1895	5.959	115.49
1900	7.090	148.11
1905	8.566	187.25
1910	10.426	234.73

The storage capacity of the reservoir is determined by using the area-volume relation curve given in Figure 4-10 below. The incremental volume between each stage elevation is determined from the above methods. As soon as the area-volume relationship has been established, preliminary design calculations to estimate the rise configuration and reservoir embamkment size can be made. Sizing of the reservoir embankment and the spillway systems will depend on the magnitude of the design runoff event and the area-volume relationship for the reservoir.

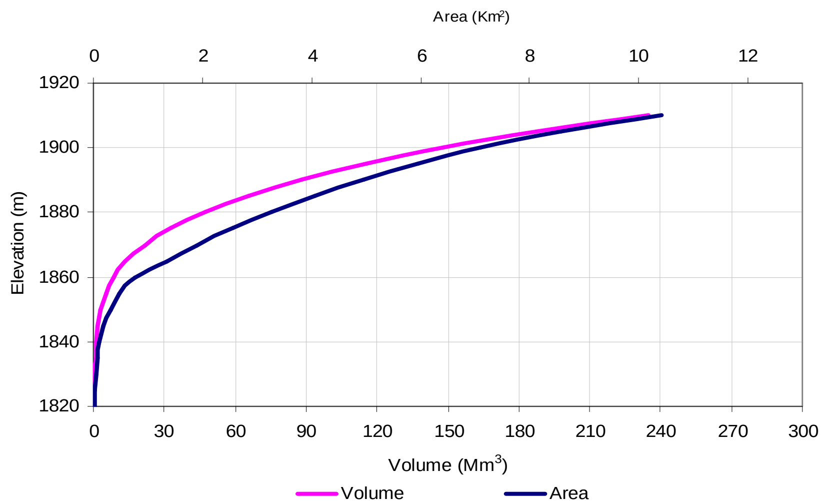

Figure 4-10: Area-volume relationship

Figure 4-11: Photographs taken from the study area at the reservoir site

3. ILWIS Script

Another way of estimating the reservoir volume is by direct calculation from ILWIS using scripts. This method is a simple method to get the volume of water that can be stored in a predefined area.. When the reservoir is constructed, the upstream part of the area will be filled up to the reservoir crest level. To determine the area that will be filled in water is estimated by using neighbourhood operations in ILWIS and it is possible also to calculate the volume of the water.

Table 4-9: Volume of the reservoir at each elevation by ILWIS calculation

Elev.	Area	Volume
1800	0.01	0.02
1805	0.01	0.06
1810	0.01	0.12
1815	0.02	0.20
1820	0.03	0.32
1825	0.04	0.48
1830	0.05	0.69
1835	0.07	0.98
1840	0.10	1.38
1845	0.17	2.01
1850	0.31	3.13
1855	0.48	5.02
1860	0.78	7.89
1865	1.34	12.85
1870	1.89	20.67
1875	2.55	31.36
1880	3.26	45.50
1885	4.06	63.42
1890	4.96	85.39
1895	5.96	112.17
1900	7.08	144.18
1905	8.51	182.37
1910	10.27	228.19

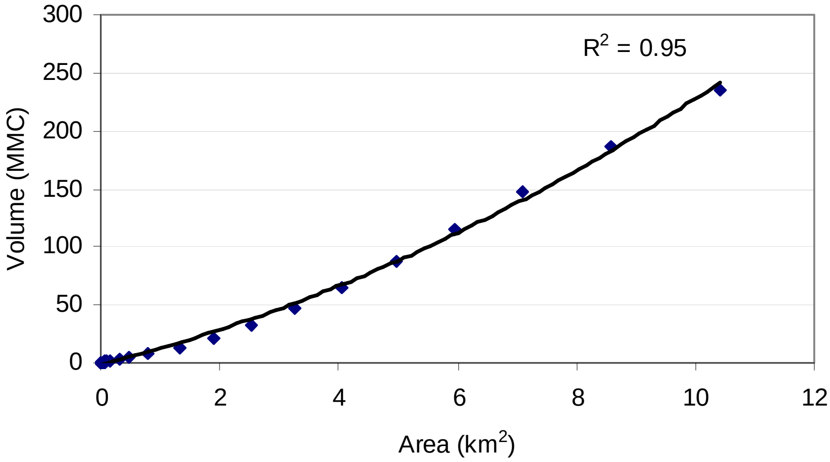

Figure 4-12: Area-volume relationship

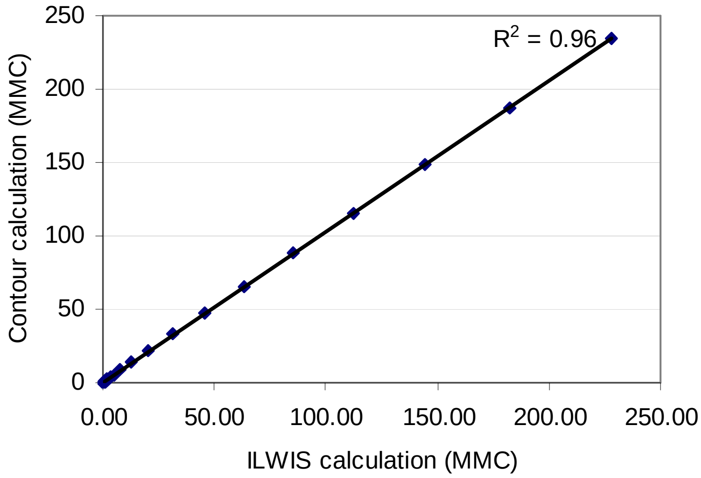

Figure 4-13: Comparison of volume in ILWIS calculation and contour calculation

The total yearly evaporation from the reservoir amounts to 14.5 Mm^3, and 15 Mm^3 of water left for environmental flow. This amount of water reduces the total water input to the reservoir both from rainfall and runoff from the catchment area. This shows that significant amount of water is evaporating from the reservoir. Though it is not possible to avoid completely part of the evaporation and the water for environment flow due to the solar radiation coming from the sun and to secure downstream inhabitants in dry season.

4.6. Irrigation Water Requirement

An important part of any evaluation of water supply and water requirements, in areas where water is a scarce commodity and seasonally variable, is to match the water supply and water requirements as closely as possible. For example, cropping systems, and areas occupied by various crops, can be manipulated to accommodate a diminishing water supply towards the end of the rainy season. Also land preparation and dates of planting can be staggered to smooth away peak water demand where it exceeds the water supply in certain months (FAO, Soil bulletin 55).

The volume of water available for irrigation will depend on hydrological studies of surface water inflow to the reservoir. The water demand for irrigation depends on studies and field work to estimate irrigation water requirements and crop production. Matching of water supply and demand involves cooperative work between water resource specialists, engineers and agriculturists (Melaku Yirga, 2003).

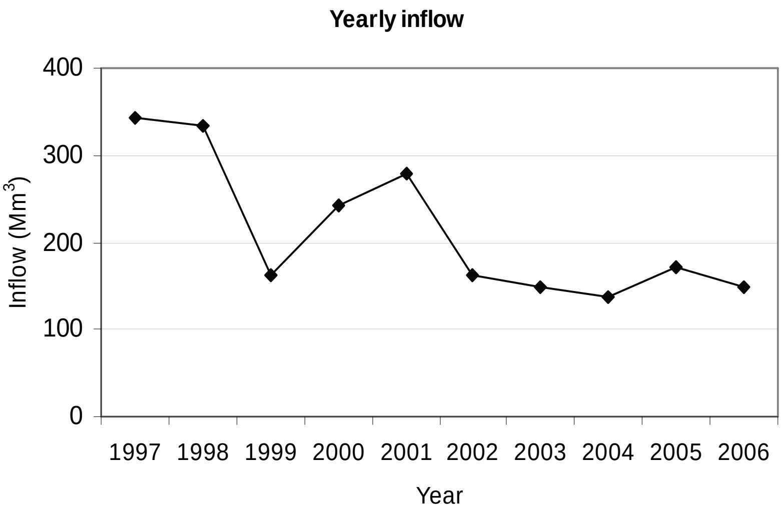

Figure 4-14: Yearly inflow to the reservoir (1997-2006)

Figure 4-14 shows the average yearly inflow to the reservoir. In this case the amount of water coming to the reservoir is 215MCM. But if we consider the amount of water coming to the reservoir in the year 2004 that is 138MCM and the difference is more than 70MCM. Care should be taken in the case of dry years like 2004 to irrigate the area properly by the reservoir operation and the crop types to be planted in this case. It is clear that if the amount of water decreases also the irrigable area will decrease and it is advisable to select which crop type is the most important for the community. It is noted that millet is most grown crop to support daily food consumption in the area.

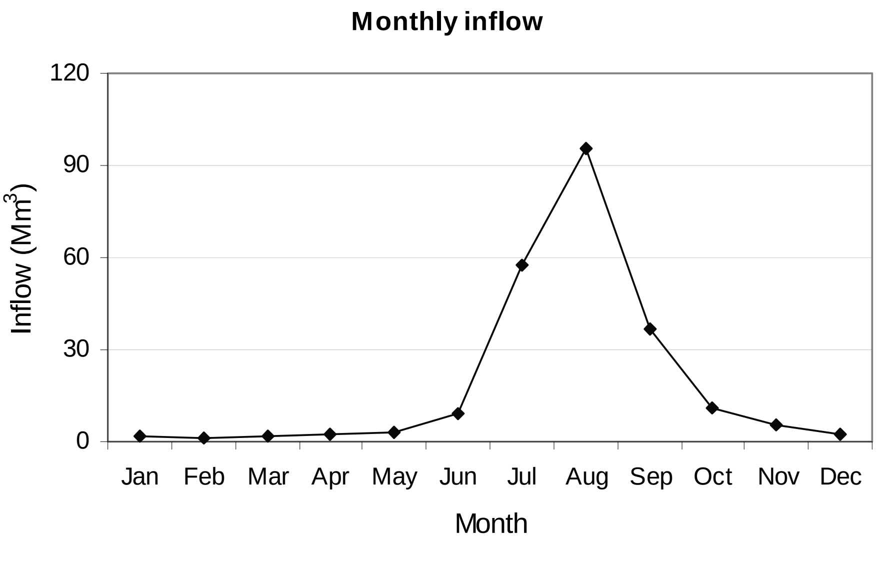

Figure 4-15: Mean monthly inflow to the reservoir (1997-2006)

The river inflow into the reservoir varies significantly from year to year. This variation is due to the variation of yearly precipitation by climatic variability in the catchment, deforestation of vegetation cover and human activities for the need of irrigable land for agriculture (due to the increase of population).

4.6.1. Crop Water Demand

Crop evapotranspiration, ETc, is calculated using crop coefficient approach by multiplying the reference crop evapotranspiration, ETo, by a crop coefficient, Kc:

$$ET_m = K_c ET_o \tag{4-5}$$

Where, *ETm* = Crop water requirement optimally (mm/d)

Kc = Crop factors (dimensionless)

ETo = Referential evapotranspiration (mm/d)

Most of the effects of the various weather conditions are incorporated into the ETo estimate. Therefore, as ETo represents an index of climatic demand, Kc varies predominately with the specific crop characteristics and only to a limited extent with climate. This enables the transfer of standard values for Kc between locations and between climates. This has been a primary reason for the global acceptance and usefulness of the crop coefficient approach and the Kc factors developed in past studies (Allen et al., 1998).

The major crops in the study area are millet, rice, teff and potato. These crops are selected due to their usage in the area and most of the farmers plant these crops for a long period of time. During field work data planting data was collected from the agricultural office. The planting period in the area is from June to September, this is because the rainy season starts at the beginning of June and ends at the end of September.

The relation described in equation 4-5 determines major crops water requirement of the study area as given in Table 4-10.

Table 4-10: Major crops, Kc value, ET_m and area weight of the crop

Major irrigated crop type	Growing Period	K_c value			Growing day	ET_m range	Area weight
		K_{ci}	K_{cmid}	K_{cend}			
Millet	Dec/Jan-April		1.2	0.35	125-130	500-800	0.4
Rice	Jan/Feb-May	1.05	1.2	0.9-0.6	150	450-650	0.2
Teff	Dec-april		1.15	0.35	130	600-800	0.2
Tomato	Dec-april		1.15	0.75	90-120	400-600	0.2

From field work data an area weight is taken as per the usage of the crop for the community in the area. Millet is the most grown crop for food preparation for most of the people and such has large weight. Due to this reasons the recommended area for millet is higher than the rest of the crops mentioned.

Table 4-11: ET_m calculation of selected crop

	Growing Period								
Description	Dec	Jan	Feb	Mar	Apr	May	ET_m total	Area Weight	Crop water requirement
K_c millet		0.40	1.20	1.20	0.35				
K_c rice		1.05	1.20	1.20	0.60	0.60			
K_c teff	0.40	1.01	1.15	1.20	0.35				
K_c tomato		1.15	1.15	0.75					
ET_o	113.88	122.29	138.11	159.43	155.25	135.04			
ET_m millet(mm)		48.92	165.74	191.32	54.34		460.31	0.40	184.12
ET_m rice(mm)		128.41	165.74	191.32	93.15	81.03	659.64	0.20	131.93
ET_m teff(mm)	45.55	123.52	158.83	191.32	54.34		573.55	0.20	114.71
ET_m tomato(mm)		140.64	158.83	119.57			419.04	0.20	83.81
ET_m total(mm)	45.55	441.48	649.13	693.52	201.83	81.03	2112.6	1.00	514.57

The ET_o is calculated using the FAO Penman–Monteith method recommended in FAO paper no. 56, which uses all parameters that govern energy exchange and corresponding latent heat flux (evapotranspiration) from uniform expanses of vegetation. Most of the parameters are calculated from weather conditions. It requires daily or monthly meteorological data including air temperature, humidity, sunshine duration and wind speed. Allen et al (1998) described that the FAO Penman–Monteith equation used for calculations of ET_o by using daily or monthly mean data can be simplified as in Equation 4-6.

$$ET_o = \frac{0.408\,\Delta(R_n - G) + \gamma\left(\frac{900}{T} + 273\right)U_2(e_s - e_a)}{\Delta + \gamma(1 + 0.34U_2)} \qquad 4\text{-}6$$

Table 4-12: Evaporation, Rainfall and Water demand for irrigation

	Jan	Feb	Mar	Apr	May	Jun	Jul	Aug	Sep	Oct	Nov	Dec
Evaporation (MCM)	1.22	1.17	1.43	1.35	1.41	1.17	0.97	1.01	1.18	1.23	1.16	1.14
Rainfall (MCM)	0.08	0.04	0.3	0.3	0.69	1.34	3.37	3.25	1.46	0.71	0.28	0.08
Water Demand (MCM)	48.5	24.7	27.3	33.6	10	0	0	0	0	8.45	12.7	3.05

4.6.2. Irrigable Area of the Study Area

The main objective of land evaluation for irrigated agriculture is to predict future conditions after development has taken place. It is necessary to forecast the benefits to the farmers and the national economy and whether these will be sustained without damage to the environment. Essentially a classification of potential suitability is required which takes account of future interactions between soils, water, crops and economic, social and political conditions.

Some factors that affect land suitability are permanent and others are changeable at a cost. The costs of necessary improvements may be determined, so that economic and environmental consequences of development can be predicted. Typical examples of permanent features are temperature, soil texture, depth to bedrock and macro-topography. Changeable characteristics which may be altered deliberately or inadvertently typically may include vegetation, salinity, depth to groundwater, micro relief, and some social and economic conditions.

Land suitability must therefore be assessed and classified with respect to specified kinds of land use i.e. cropping, irrigation and management systems. It is obvious that the requirements of crops and irrigation and management methods differ, so the suitability of any land unit may be classed differently for various uses. It can be useless or misleading to indicate suitability for irrigated agriculture in general if the land developer needs to know about its potential for a specific irrigated crop or irrigation method.

The physical, soil, topography, drainage, climate and water quality factor are inter related. These factors influence the required crop production inputs and yield outputs, which intern are controlled by technological levels, economic conditions, social organization, resource fullness of people, and the goals of the development. Irrigation planning can be accomplished by using the land classification survey as a systematic, integrating process for many of these plan determining elements. Multi-discipline experts can study these plan determining elements.

Considering topography of the area, provisional irrigable area was identified and it is estimated as about 20000 hectares. In order to identify irrigable area by topographical methods, a slope map of the area of study is created from the digital elevation map. For gravity irrigation the slope limit should be from 0.2% to 2%-3% (FAO guide lines for soil description and standards for the classification of land for irrigation in the province of Alberta). To avoid or minimize drainage problems the lower limit of slope is set to 0.2%. The upper limit is set to 3% for gravity flow, irrigation is important to flow the water by gravity with out any driving force or pumping from the source to the command area. As indicated above, in general the selection of lands is phased in to two parts: The selection of arable land on the basis of farm production, and selection of the irrigable area on the basis of the economics of the project plan, where in irrigation benefits determined by economic evaluation equal or exceed project irrigation costs. Taking this slope limit in consideration the map in Figure 4-16 produces that match with the slope limit.

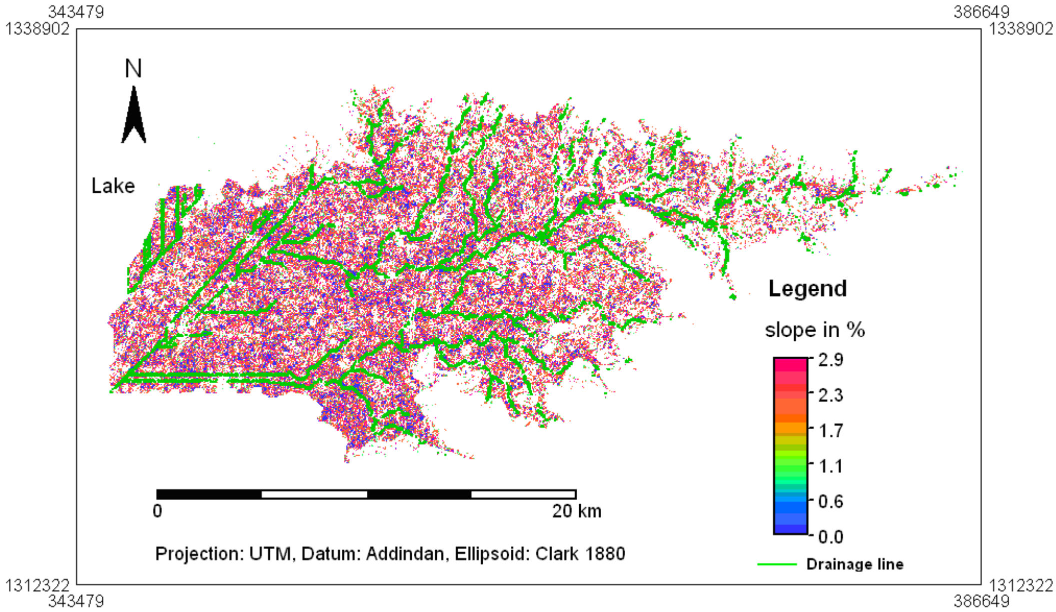

Figure 4-16: Irrigable area with slope lower than 3% and larger than 0.2%

The irrigable area for the catchment is located above the gauging station in Addis Zemen and the flood plain is ungauged and it is very suitable for irrigation. In Figure 4-17 the estimated area of the catchment for gauged and for total Ribb is given in slope percentage.

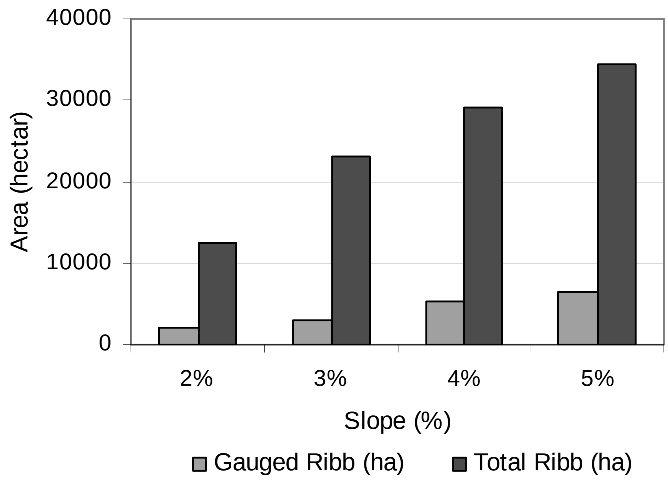

Figure 4-17: Irrigable area for gauged Ribb and total Ribb catchment

Net irrigation need = crop water requirement = 514mm
Overall efficiency = 65% (for semi-arid area between 60%-70%)
Gross irrigation need = Net irrigation need/overall efficiency = 790mm

From Table 4-11 crop water requirement of the crop we can estimate the command area and it lies in the south-west side of the reservoir outlet. The reservoir will irrigate 17,000 ha to 20,000ha of land.

Table 4-13: The water balance components and irrigable area

Evaporation (MCM)	Rainfall (MCM)	River Inflow (MCM)	Environmental flow (MCM)	Storage capacity (MCM)	Irrigable Area (ha)
14.5	12	215	15	168	17000-20000

4.7. Environmental Flow

Water is essential to all kinds of human development and livelihood support systems including ecosystems management. However, water resources are now under pressure due to increased competing demands and global warming, which have led to complex water management challenges. In Africa, longer dry seasons and more uncertain rainfall are attributed to global warming (IPCC, 2007) and it is anticipated that there will be a 10–20% decrease in river flows over some regions at mid- latitudes and in the dry tropics, some of which are presently water stressed areas. This is threatening the efforts towards environmental flows (EF) provisions in many rivers, particularly in water stressed areas. Despite that there are many challenges towards sustainable water resource management which includes the assessment and the understanding of how much water can be taken from a river before its ability to meet social, ecological and economic needs is hindered. Another challenge is on how to estimate the ecological reserves and the mechanisms for allocation of water for highly regulated river as is the case for the Ribb River, while ensuring the water dependant livelihoods of the poor are not affected (Kashaigili et al., 2007). In this study the environmental flow is estimated based on the historical series mean monthly flows of the Ribb River.

Table 4-14: Environmental flow for Ribb river

	Jan	Feb	Mar	Apr	May	Jun	Jul	Aug	Sep	Oct	Nov	Dec
Average flow (m^3/s)	0.96	0.63	0.5	0.64	0.66	-	-	-	-	3.96	2.91	1.15
Release (m^3/s)	0.48	0.31	0.25	0.32	0.33	-	-	-	-	1.98	1.46	0.57

Environmental flow is estimated based on 50% of the historical series mean monthly flow of the river for dry seasons (the flow is taken as 25%-50% by considering the amount of available flow). In the rainy season there is no need of releasing environmental flow due to the rain which is covering downstream of the reservoir.

5. Water Balance

5.1. Water Balance Components

The water balance for Ribb reservoir was determined for the years 1997 to 2006 on a monthly basis. Monthly data for precipitation, evaporation, stream flow and expected reservoir release were used for modelling of the reservoir water balance.

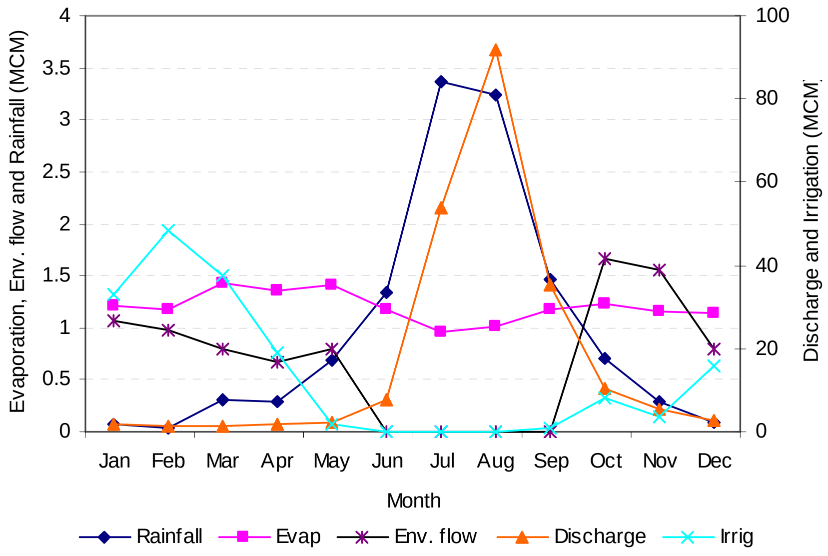

Figure 5-1: The water balance components of the reservoir

The inflow components are stream flow to the reservoir and precipitation, while the outflow components are water required for irrigation, evaporation and the water required for environmental flow. Precipitation and evaporation converted into volume using the reservoir area and the discharge converted to volume by changing the daily record to annually.

Results for the wet season, shows that the reservoir level declines starting from the month of November and continue decreasing until the rainfall starts in the month of April. The largest amount of input water from surface runoff from the catchment is in the month of July and August to balance the outflow demand for irrigation during the dry season. The reservoir storage capacity follows more the pattern of the surface runoff and precipitation. This is because when the rainfall over the catchment becomes high the river discharge becomes high. It should be noted that the rainfall input indicated on the Figure is rain that falls over the reservoir area. Even though months of May and September seems to have the same amount of input from surface runoff and precipitation and comparable output in terms of evaporation the change in volume is higher in September than in May. Because September was gaining water from streams of the catchment, since it is the end of the wet season, where as in May the reservoir doesn't have any streams which drains to the reservoir. Because May is the end of the dry and the beginning of the wet period that rainfall which is high in May is taken to compensate the slightly higher evaporation and large amount of shortage of surface runoff. The average yearly amount of water given in Table 5-1 shows that change in storage is positive. But, in dry year change in storage will be negative due to the decreasing of river flow and rainfall.

Table 5-1: The annual average water balance components of the reservoir

Water balance components	Amount of water per year (MCM)
River inflow	+215
Irrigation demand	-168
Evaporation	-14.5
Rainfall	+12
Environmental flow	-15
Change in storage	+29.5

5.2. Sensitivity Analysis

In modelling any calibration is unique on itself but, it must also be realized, on the other hand non-unique with respect to the many other approaches that also may yield an equally calibration result. The main purpose of a sensitivity analysis is to quantify how sensitive the model is to certain changes in the input data and as such, a sensitivity analysis basically is a procedure to quantify on the uncertainty of the calibrated model. There are uncertainties at the time of measurement and computation due to human, instrument and shortage of data. During calibration of the reservoir water balance model, sensitivity analysis has to be executed to understand to which variable the model is more sensitive and estimate the variation on the output parameter that could arise due to uncertainties in the sensitive variable.

Sensitivity analysis has been made to all variables considered in the lake water balance. As it is indicated in fig 5-2, the model is more sensitive to river inflow and outflow for irrigation. 10 % change in the river inflow can cause up to 20Mmc of water on average in the reservoir volume. Similarly by changing outflow for irrigation by 10% there will be a change loose and gain up to 15Mmc of water on the reservoir volume. The variable to which the model is least sensitive is open water evaporation due to the lesser area coverage on the ground as compared to the catchment area.

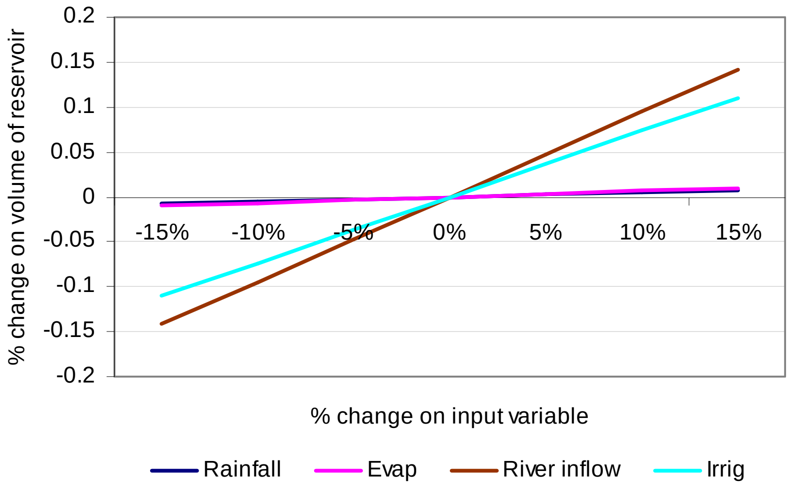

Figure 5-2: Sensitivity analysis of the reservoir

6. Conclusion and Recommendation

6.1. Conclusion

The reservoir water balance for Ribb reservoir was modelled by hydrological model called HBV-96. The model is selected for its suitability for the area of high topographic variability and the data availability for the model. In HBV-96 the discharge of the catchment is simulated by using rainfall, temperature and evaporation data. Land classes considered for runoff simulation are forest and field (non forest) areas.

Runoff data measured on the outlet of the river is used for calibration and validation. This model has been applied successfully in Lake Tana basin catchments that have similar characteristics of Ribb reservoir Catchment. This model simulated runoff in the catchment with a relative volume error of 4% and Nash and Sutcliff (R^2) of 0.8. The components for water balance of the reservoir are computed by spread sheet model developed for this study. These components are runoff from the catchment, areal rainfall, open water evaporation, water demand for irrigation and environmental water release.

The catchment parameters needed by HBV-96 model were extracted by remote sensing image using GIS software. The measurement data taken from ground truth were used with the data acquired from remote sensing images. Ribb reservoir catchment area, sub basins of the catchment with their catchment area and outlet coordinates, elevation zones and land cover information were the parameters extracted for the HBV-96 model from remote sensing and GIS. The reservoir area contour was generated from ASTER image. The storage capacity of the reservoir was done in ILWIS software.

The HBV-96 model is calibrated by using the steps described in the manual. The parameters in the model have free ranges to calibrate the most selected parameters starting from the initial state to the optimum value of the parameters. Validation was done from the parameters obtained from the calibration.

The storage capacity of the reservoir calculated using the contour lines of ASTER DEM is amounting 148Mm^3. This shows that remote sensing can be considered as an alternative method, if there is a need to evaluate the storage capacity in conditions when data is not available.

Downstream flooding occurred in Fogera flood plain which is the down stream part of Ribb catchment and Gumera catchment. This flooding is not only caused by Ribb river, but also Gumera river and back water effects of high Lake level. From the Ribb river the amount of flooding reduced by 168 MMC of water and from the total flooding the reservoir reduces the amount of flood in some extent.

The water balance model for the reservoir shows that the annual runoff from the catchment to the Ribb reservoir is 215 million m^3 based on the discharge data. With additional 12 million m^3 from the rainfall, the annual inflow to the reservoir is 227 million m^3. The region is semi-arid and the rainfall is high in wet season, so that it replenishes the soil moisture to its water holding capacity. Therefore, total runoff from the catchment depends on the direct runoff and rainfall.

Actual evapotranspiration depends on the supply of water for irrigation on the growing period. The average potential amount of water for the irrigation is estimated to be 168 million m^3. But, in dry years the amount of water will decrease from this amount used for the irrigation. Due to this reason there will be a scarcity of water for the irrigation in dry years. So, water is a limiting constraint to agriculture production in the Ribb irrigation command area. Therefore, it is necessary to reselect crops to irrigate in dry years.

The sensitivity analysis shows the volume of the reservoir is sensitive to all water balance components. But, most sensitive to river inflow to the reservoir and outflow for irrigation water demand.

6.2. Recommendation

Estimation of sediment load determines the useful life of the reservoir. Sediment data is required in order to establish the potential loss of capacity in Ribb reservoir due to sedimentation over the design life of the project. Observation techniques permit sampling of suspended sediment, although bed load sampling is possible but it is very inaccurate. There is also seasonal effect, with sediment load in the early wet months (June and July) higher than those on later months (August and September) for the same discharge.

A further study should be taken to estimate the water balance of the reservoir after the construction of the reservoir is completed with the help of recorded water level data from the reservoir. This method is more accurate than this work used due to the lack of recorded water level data.

References:

Abeyou, W., 2008. Hydrological balance of Lake Tana upper Blue Nile basin, Ethiopia, ITC, Enschede, 94 pp.

Allen, R.G., Pereira, L.S., Raes, D. and Smith, M., 1998. Crop evapotranspiration-Guidelines for computing crop water requirements-FAO Irrigation and drainage paper 56. FAO, Rome, 300.

Baipeng, L., Qin, Y., Chunquan, C. and Yanliang, W., 2007. The Accuracy assessment Experiment of ASTER 3D Ortho Product in Beijing, China.

Bergström, S. and Graham, L.P., 1998. On the scale problem in hydrological modelling. Journal of Hydrology, 211(1-4): 253-265.

Cherie Mekonnen, S., 2005. Assessment of catchment water balance using GIS and remote sensing : Roxo, Portugal, ITC, Enschede, 109 pp.

Clarke, D., Smith, M. and El-Askari, K., 1998. CropWat for Windows: User Guide. Version, 4: 0013.

Dingman, S.L., 1994. Physical hydrology Prentice Hall, Upper Saddle River, 568 pp.

Doll, P. and Siebert, S., 2002. Global modeling of irrigation water requirements. Water Resources Research, 38(4): 8-8.

FAO, Soil bulletin 55. 1985;Guide lines, land evaluation for irrigated agriculture. Rome, Italy; Food and Agricultural Organization of the United Nations.

Gebreegziabher, Y., 2005. Assessment of the water balance of lake Awassa catchment, Ethiopia, ITC, Enschede, 92 pp.

Goel, M.K., Kumar, P., Jain, S.K. and Tiwari, R.S., 2007. Operation analysis of a reservoir in GIS environment using remote sensing inputs. Int. J. Remote Sens., 28(2): 335-352.

IPCC, 2007. IPCC (Intergovernmental Panel on Climate Change). Climate Change : Impacts, Adaptation and Vulnerability. Working Group II Contribution to the. Intergovernmental Panel on Climate Change,Fourth Assessment Report. www.ipcc.ch/SPM13apr07.pdf (accessed 30.05.2007).

Kashaigili, J.J., McCartney, M. and Mahoo, H.F., 2007. Estimation of environmental flows in the Great Ruaha River Catchment, Tanzania. Physics and Chemistry of the Earth, Parts A/B/C, 32(15-18): 1007-1014.

Kebede, S., Travi, Y., Alemayehu, T. and Marc, V., 2006. Water balance of Lake Tana and its sensitivity to fluctuations in rainfall, Blue Nile basin, Ethiopia. Journal of Hydrology, 316(1-4): 233-247.

Lee, H., McIntyre, N., Wheater, H. and Young, A., 2005. Selection of conceptual models for regionalisation of the rainfall-runoff relationship. Journal of Hydrology, 312(1-4): 125-147.

Lindström, G., Johansson, B., Persson, M., Gardelin, M. and Bergström, S., 1997. Development and test of the distributed HBV-96 hydrological model. Journal of Hydrology, 201(1-4): 272-288.

Maidment, D.R.e., 1993. Handbook of hydrology. McGraw-Hill, New York etc., 650 pp.

Melaku Yirga, W., 2003. Assessment of irrigation potential in the Roxo dam area, Portugal, for strategic planning using GIS - RS, ITC, Enschede, 102 pp.

Nash, J.E. and Sutcliffe, J.V., 1970. River flow forecasting through conceptual models : part I. a discussion of principles. Journal of hydrology, 10(3).

Refsgaard, J.C. and Knudsen, J., 1996. Operational validation and intercomparison of different types of hydrological models. Water Resources Research 32(7): 2189-2202.

Rientjes, T.H.M., 2007. Modelling in hydrology. Department of water resources, ITC, Enschede.

Smakhtin, V., Revenga, C. and Doell, P., 2004. Taking into Account Environmental Water Requirements in Global-scale Water Resources Assessments. Book.

SMHI, 2006. Integrated Hydrological Modelling System Manual. Version 5.10.

Smith, M., 1996. CROPWAT: a computer program for irrigation planning and management.

Uhlenbrook, S. and Leibundgut, C., 2000. Development and validation of a process oriented catchment model based on dominating runoff generation processes. Physics and Chemistry of the Earth, Part B: Hydrology, Oceans and Atmosphere, 25(7-8): 653-657.

UNEP, 2000. Global Environmental Outlook, United Nations Environmental Programme’s.

Vallet-Coulomb, C., Legesse, D., Gasse, F., Travi, Y. and Chernet, T., 2001. Lake evaporation estimates in tropical Africa (Lake Ziway, Ethiopia). Journal of Hydrology, 245(1-4): 1-18.

Vijay, R. and Sasikumar, M.S., 2003. Computation Of Reservoir Capacity: A GIS Based Approach. Allied Publishers.

Winter, T.C., 1981. Uncertainties in Estimating the Water Balance of Lakes. Water resources Bulletin 17,No.1:82-115.

WWAP, 2003. From Potential Conflict to Co-operation Potential: Water for Peace: UNESCO, Paris.

Annex:

Appendix 1: Monthly Relative Humidity

Year	Jan	Feb	Mar	Apr	May	Jun	Jul	Aug	Sep	Oct	Nov	Dec
1997	42	45	52	57	68	77	87	85	74	76	74	62
1998	55	42	50	46	64	74	90	90	82	73	50	39
1999	45	31	39	46	60	68	87	83	78	80	52	56
2000	44	41	47	66	62	74	85	86	80	82	67	60
2001	47	43	45	44	58	80	88	90	76	70	59	54
2002	53	44	49	45	49	74	81	81	66	49	47	50
2003	35	37	42	35	33	68	85	84	76	59	48	44
2004	42	40	34	47	42	72	83	84	78	66	62	52
2005	42	30	42	37	43	68	86	81	82	71	56	34
2006	31	33	33	42	61	70	82	71	78	48	41	43
2007	39	37	33	44	51	75	85	80	73	55	45	34

Appendix 2: Monthly sunshine hours

Year	Jan	Feb	Mar	Apr	May	Jun	Jul	Aug	Sep	Oct	Nov	Dec
1997	8.01	8.03	6.82	6.89	5.96	4.87	4.09	4.08	6.33	6.15	7.10	7.90
1998	8.53	8.91	8.00	8.62	7.55	7.19	2.94	3.21	5.64	7.42	8.94	9.50
1999	8.35	9.42	9.19	10.86	7.59	6.10	3.71	4.22	5.96	6.55	8.88	8.63
2000	9.15	9.13	9.10	6.43	7.83	6.85	4.31	3.62	5.83	6.54	8.44	8.61
2001	9.10	8.57	7.00	8.18	8.02	5.49	3.68	3.43	6.29	7.38	8.41	8.72
2002	8.18	8.75	7.83	9.08	8.75	6.50	5.10	4.40	6.23	7.90	8.37	8.94
2003	8.97	7.86	7.99	7.73	7.91	6.15	4.24	3.39	5.73	7.48	8.41	8.75
2004	7.59	9.01	8.80	5.98	8.37	4.48	5.91	5.28	5.69	7.42	8.51	9.16
2005	6.45	7.84	8.02	5.79	6.48	5.41	4.95	4.37	5.44	7.58	8.52	9.57
2006	8.73	6.58	7.32	5.34	4.31	6.22	4.15	3.39	5.01	7.81	8.50	8.51
2007	8.18	7.84	8.48	7.84	7.24	5.81	3.19	4.00	5.12	7.76	8.23	9.12

Appendix 3: Monthly wind speed

Year	Jan	Feb	Mar	Apr	May	Jun	Jul	Aug	Sep	Oct	Nov	Dec
1997	1.07	1.31	1.28	1.30	1.27	1.23	1.13	1.25	1.15	0.81	0.95	1.02
1998	1.05	1.06	1.27	1.46	1.28	1.25	1.17	1.27	1.14	0.85	0.97	1.04
1999	1.12	1.46	1.21	1.50	1.43	1.41	1.08	1.43	1.27	0.84	1.06	0.99
2000	1.30	1.35	1.37	1.43	1.26	1.15	1.19	1.23	0.93	0.70	0.74	0.89
2001	1.09	1.21	1.23	1.33	1.10	1.11	1.15	1.09	1.24	0.89	1.00	1.16
2002	1.49	1.35	1.41	1.73	1.33	1.31	1.35	1.33	1.11	1.00	1.08	1.13
2003	1.20	1.25	1.35	1.51	1.75	1.23	1.06	1.20	1.04	0.88	1.03	1.10
2004	1.00	1.24	1.25	1.13	1.64	1.23	1.18	1.13	1.02	0.74	0.78	1.00
2005	1.02	1.21	1.15	1.25	1.37	1.42	1.10	1.36	1.24	0.81	0.89	1.06
2006	1.12	1.19	1.22	1.21	1.19	1.07	1.06	1.09	0.95	0.78	0.91	1.09
2007	0.90	1.01	1.20	1.17	1.11	0.87	0.95	1.17	1.04	0.98	1.01	1.32

Appendix 4: Monthly rainfall

Year	Jan	Feb	Mar	Apr	May	Jun	Jul	Aug	Sep	Oct	Nov	Dec
1997	0.11	0.00	2.27	1.55	6.37	7.11	13.36	12.31	6.63	9.87	0.48	2.66
1998	0.44	0.00	0.68	0.23	6.57	4.09	12.95	13.28	8.21	2.45	0.02	0.00
1999	1.12	0.00	0.00	0.32	1.43	5.93	14.75	11.89	5.83	9.09	0.38	0.63
2000	0.00	0.02	0.22	4.04	2.42	5.64	13.43	14.23	8.54	4.45	1.31	0.02
2001	0.00	0.05	0.71	0.80	3.08	6.58	16.02	13.23	6.16	1.94	0.15	0.23
2002	0.01	0.00	1.93	1.52	1.52	6.78	8.17	9.85	5.41	0.25	0.53	0.61
2003	0.00	0.50	0.82	0.62	0.63	2.90	13.71	12.71	7.27	1.22	1.11	0.48
2004	0.02	1.30	1.09	2.52	0.62	4.70	10.76	9.52	4.03	2.77	1.42	0.41
2005	0.04	0.00	1.10	0.34	1.82	7.48	15.28	14.06	7.21	0.16	0.99	0.00
2006	0.00	0.05	0.22	2.11	4.75	5.67	15.55	14.60	8.50	1.53	0.00	0.25
2007	0.64	0.02	0.72	2.93	2.12	9.43	13.70	15.15	6.76	0.80	0.00	0.00

Appendix 5: Monthly maximum temperature

Year	Jan	Feb	Mar	Apr	May	Jun	Jul	Aug	Sep	Oct	Nov	Dec
1997	22.0	23.5	24.0	23.0	22.0	20.6	18.3	19.2	21.4	21.0	21.9	21.2
1998	23.0	24.1	24.9	26.5	23.2	22.2	17.7	17.9	19.8	20.8	22.1	22.6
1999	22.3	24.9	24.9	25.3	24.6	23.4	17.5	18.2	19.9	19.4	21.5	22.2
2000	22.8	24.4	25.5	22.8	23.7	22.2	19.0	18.7	19.8	19.8	21.4	22.6
2001	22.8	25.0	24.1	25.3	23.5	20.1	18.3	18.3	20.4	21.8	22.2	22.8
2002	22.9	25.1	24.6	24.9	25.5	22.1	20.2	19.7	20.4	22.9	23.1	22.9
2003	23.7	24.5	24.5	25.4	26.0	22.4	18.5	18.8	20.1	21.9	22.3	22.4
2004	23.7	23.9	25.0	23.2	25.9	21.8	19.6	19.3	20.9	21.4	22.3	22.4
2005	22.8	25.9	24.9	25.5	24.6	23.1	18.1	19.6	20.2	21.6	22.4	22.7
2006	23.7	25.1	25.2	24.4	22.6	21.6	19.5	19.3	20.7	22.8	22.4	22.5
2007	22.6	24.5	26.0	24.9	24.7	20.9	18.1	19.2	20.5	21.5	22.5	22.6

Appendix 6: Monthly minimum temperature

Year	Jan	Feb	Mar	Apr	May	Jun	Jul	Aug	Sep	Oct	Nov	Dec
1997	8.0	8.5	10.9	10.8	10.6	10.5	10.4	10.3	9.8	9.1	8.5	9.5
1998	8.8	9.2	11.3	13.0	12.2	10.9	10.6	10.5	9.8	9.3	7.3	6.7
1999	8.0	9.7	9.4	11.3	10.8	10.3	10.0	10.1	9.0	9.3	7.0	7.7
2000	7.9	9.0	10.2	10.1	10.8	10.1	9.8	9.8	9.2	9.1	8.2	7.6
2001	6.9	9.5	10.6	11.5	11.7	10.3	10.1	10.4	9.0	9.1	7.4	8.0
2002	7.7	9.2	10.5	10.5	11.9	10.5	10.0	9.6	9.0	7.7	7.8	7.4
2003	7.3	9.3	10.5	10.9	12.2	10.7	9.3	9.5	9.1	8.4	8.1	7.9
2004	8.7	8.3	10.7	11.2	11.1	10.3	9.9	9.8	9.1	7.6	7.9	7.9
2005	7.4	10.2	10.5	12.0	11.4	10.7	9.6	8.8	9.5	8.5	7.5	6.9
2006	8.5	9.9	10.7	10.5	10.4	10.3	10.4	10.3	9.5	9.3	8.0	7.5
2007	8.2	9.5	10.7	11.1	11.6	10.9	10.5	10.1	9.7	7.9	7.5	7.4

Appendix 7: Contour lines at different elevation

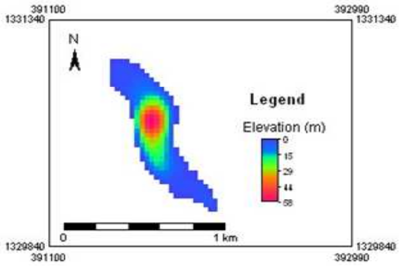

1850m

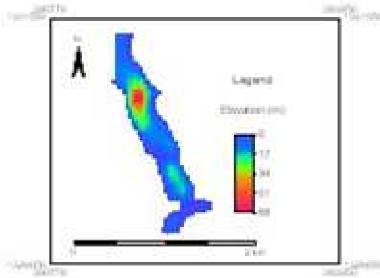

1860m

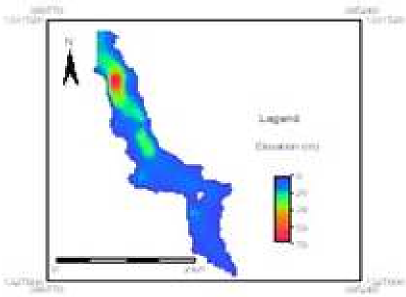

1870m

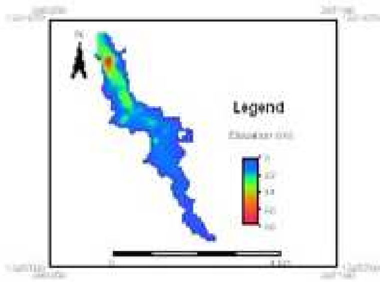

1880m

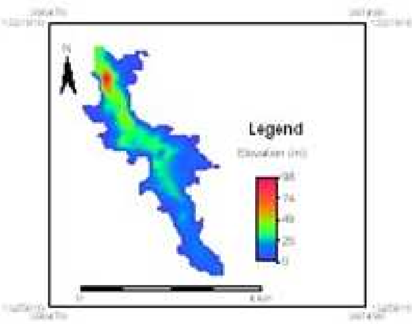

1890m

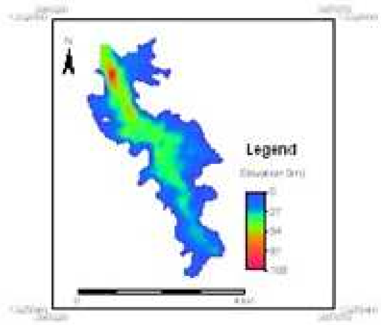

1910m

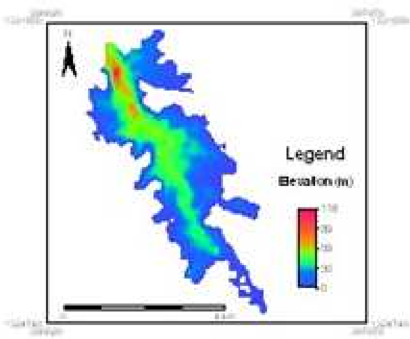

1910m

Contour line of the reservoir at different elevation

Appendix 8: Photographs taken from the study area